Redox Biology 52 (2022) 102322

Contents lists available at ScienceDirect

Redox Biology

journal homepage: www.elsevier.com/locate/redox

Overexpression of NAG-1/GDF15 prevents hepatic steatosis through inhibiting oxidative stress-mediated dsDNA release and AIM2 inflammasome activation

Ying Wang [a], Chaojie Chen [a], Jiajun Chen [a], Tingting Sang [a], He Peng [a], Xiaojian Lin [a], Qian Zhao [a], Shengjia Chen [a], Thomas Eling [b], Xingya Wang [a,*]

[a] School of Pharmaceutical Sciences, Zhejiang Chinese Medical University, Hangzhou, 311400, China
[b] National Institute of Environmental Health Science, Research Triangle Park, NC, 27709, USA

ARTICLE INFO

Keywords:
NAG-1/GDF15
Hepatic steatosis
Lipid metabolism
AIM2 inflammasome
ROS
dsDNA

ABSTRACT

Mitochondrial dysfunction and oxidative stress-mediated inflammasome activation play critical roles in the pathogenesis of the non-alcoholic fatty liver disease (NAFLD). Non-steroidal anti-inflammatory drug (NSAID)-activated gene-1 (NAG-1), or growth differentiation factor-15 (GDF15), is associated with many biological processes and diseases, including NAFLD. However, the role of NAG-1/GDF15 in regulating oxidative stress and whether this process is associated with absent in melanoma 2 (AIM2) inflammasome activation in NAFLD are unknown. In this study, we revealed that NAG-1/GDF15 is significantly downregulated in liver tissues of patients with steatosis compared to normal livers using the Gene Expression Omnibus (GEO) database, and in free fatty acids (FFA, oleic acid/palmitic acid, 2:1)-induced HepG2 and Huh-7 cellular steatosis models. Overexpression of NAG-1/GDF15 in transgenic (Tg) mice significantly alleviated HFD-induced obesity and hepatic steatosis, improved lipid homeostasis, enhanced fatty acid β-oxidation and lipolysis, inhibited fatty acid synthesis and uptake, and inhibited AIM2 inflammasome activation and the secretion of IL-18 and IL-1β, as compared to their wild-type (WT) littermates without reducing food intake. Furthermore, NAG-1/GDF15 overexpression attenuated FFA-induced triglyceride (TG) accumulation, lipid metabolism deregulation, and AIM2 inflammasome activation in hepatic steatotic cells, while knockdown of NAG-1/GDF15 demonstrated opposite effects. Moreover, NAG-1/GDF15 overexpression inhibited HFD- and FFA-induced oxidative stress and mitochondrial damage which in turn reduced double-strand DNA (dsDNA) release into the cytosol, while NAG-1/GDF15 siRNA showed opposite effects. The reduced ROS production and dsDNA release may be responsible for attenuated AIM2 activation by NAG-1/GDF15 upon fatty acid overload. In conclusion, our results provide evidence that other than regulating lipid homeostasis, NAG-1/GDF15 protects against hepatic steatosis through a novel mechanism via suppressing oxidative stress, mitochondrial damage, dsDNA release, and AIM2 inflammasome activation.

1. Introduction

NAFLD is a prevalent chronic disease worldwide and has become an emerging health threat in recent years, which comprises a wide disease spectrum ranging from hepatic steatosis to more severe diseases including non-alcoholic steatohepatitis (NASH), fibrosis, cirrhosis, and hepatic carcinoma [1]. The mechanisms underlying the progression from steatosis to NASH or more advanced disease stages are still poorly understood. Recently, the "multiple hit" mechanisms which state that simple steatosis can lead to the development of severe NAFLD through multiple events have been proposed including insulin resistance, mitochondrial dysfunction, adipose tissue dysfunction, oxidative stress, endoplasmic reticulum (ER) stress, altered regulation of innate immunity, or compositional changes of microbiota [2]. Among these factors, oxidative stress which increases ROS production is considered "an important hit" to trigger progression from simple steatosis to NASH [3,4].

Hepatic steatosis or fatty liver, the most predominant form of NAFLD, is defined as an increased accumulation of lipids in hepatocytes of at least 5% of liver weight and results from the disruption of hepatic

* Corresponding author. School of Pharmaceutical Sciences, Zhejiang Chinese Medical University, 260 Baichuan Road, Hangzhou, 311400, China.
E-mail address: xywang@zcmu.edu.cn (X. Wang).

https://doi.org/10.1016/j.redox.2022.102322
Received 28 February 2022; Received in revised form 10 April 2022; Accepted 23 April 2022
Available online 27 April 2022

lipid homeostasis along with the accumulation of triglyceride (TG) or fatty acids [5]. FFAs were proposed to act as lipotoxic triggers that generate ROS and cause mitochondrial damage, which results in the progression from simple steatosis to more severe NAFLD stages [6,7]. Animal studies showed that hepatic lipids composed of saturated fatty acids are primarily responsible for hepatic lipotoxicity during NAFLD [8]. Although numerous studies identified multiple therapeutic targets for the treatment of NAFLD, there are currently no approved drug treatments for NASH [9]. Therefore, early intervention via regulating lipid homeostasis and ROS production and thus inhibiting steatosis is critical in the prevention of NASH and more advanced liver diseases.

NAG-1/GDF15, a cell stress-response cytokine, is a distinct member of the transforming growth factor-beta (TGF-β) superfamily [10]. NAG-1/GDF15 is widely expressed in various tissues with the highest levels in the liver and placenta [11,12]. NAG-1/GDF15 has been implicated in many pathological diseases including obesity, cardiovascular diseases, renal failures, diabetes, and cancer, probably through paracrine/autocrine pathways [10,13–15]. Elevated plasma NAG-1/GDF15 levels have been reported in human subjects with these diseases [16–19] and chronic liver diseases [20,21], suggesting NAG-1/GDF15 may serve as a potential diagnostic biomarker for these diseases. It has been reported that the plasma level of NAG-1/GDF15 was significantly higher in human subjects with obesity or higher body mass index (BMI) [17,22,23].

However, contradictory results reported that the serum level of NAG-1/GDF15 was inversely correlated with BMI in pregnant women [24], and human monozygotic twins [25]. Emerging evidence, including our previous study, has indicated that treatment or overexpression of NAG-1/GDF15 exerts protective effects against obesity and insulin resistance in mice and primates [26–31]. Therefore, the exact functional role of NAG-1/GDF15 in the development and progression of obesity-related diseases is largely unknown. Recently, increased serum level of NAG-1/GDF15 has also been reported in human NASH subjects with advanced fibrosis [32]. Using genetic approaches, several studies showed that NAG-1/GDF15 exhibited protective effects against hepatic steatosis, inflammation, fibrosis, liver injury, and NASH in mouse models [33–36]. However, the exact role and the underlying molecular mechanisms of NAG-1/GDF15 in hepatic steatosis are still unknown.

Recently, emerging evidence has pointed to the critical roles of the inflammasomes in regulating autoimmune and metabolic diseases [37]. The AIM2 inflammasome belongs to the interferon-inducible gene HIN-200 domain-containing protein family and structurally consists of an N-terminal pyrin domain (PYD) and a C-terminal oligonucleotide-binding HIN domain. Upon activation, AIM2 recruits apoptosis speck-like protein (ASC) and caspase-1 to form a molecular platform for the maturation and secretion of IL-1β and IL-18 [38]. The AIM2 inflammasome has been reported to play a key role in viral infections and has also been characterized in autoimmune, inflammatory, and metabolic diseases such as dermatitis, arthritis, cancers, and cardiovascular diseases [39–41]. However, the role of the AIM2 inflammasome and its physiological relevance to NAFLD are poorly understood. At present, several studies have reported that AIM2 inflammasome activation may contribute to the progression of steatosis to NASH [42–44]. However, the specific role of AIM2 inflammasome in steatosis and whether it can be regulated by NAG-1/GDF15 has never been reported.

Therefore, the present study aimed to examine whether NAG-1/GDF15 is protective against HFD or FFA overload-induced-steatosis *in vivo* and *in vitro* and whether the anti-steatotic effect of NAG-1/GDF15 is mediated via AIM2 inflammasome activation. This study was also aimed to investigate the molecular mechanisms of how NAG-1/GDF15 inhibited AIM2 inflammasome activation using genetic approaches. Our study demonstrates that NAG-1/GDF15 has a potential role in the treatment of obesity-induced NAFLD, which may through regulating fatty acid metabolism, inhibiting ROS overproduction, reducing mitochondrial damage, and dsDNA release, and thus inhibiting AIM2 inflammasome activation.

2. Materials and methods

2.1. Materials

Dulbecco's modified Eagle's medium (DMEM) and penicillin-streptomycin solution were purchased from Gibco (Grand Island, NY, USA). Fetal bovine serum (FBS) was obtained from Gemini (Grand Island, NY, USA). Oleic acid (OA), palmitic acid (PA), and 4, 6-Diamidino-2-phenylindole (DAPI) were purchased from Sigma-Aldrich (St. Louis, MO, USA). [3-(4, 5-dimethylthia-zol-2-yl)-2, 5-diphenyltetrazolium bromide] (MTT) was obtained from AMRESCO (Solon, OH, USA). Bodipy 493/503, Lipofectamin® 2000 reagent, and Quant-iT PicoGreen dsDNA assay kit were purchased from Thermo Fisher Scientific (Waltham, MA, USA). Oil Red O dye was purchased from Solarbio Science & Technology (Beijing, China). The enzyme-linked immunosorbent assay (ELISA) kits (human GDF15 (#DGD150), mIL-1β (#MLB00C), and mIL-18 (#7625)) were obtained from R&D Systems (Minneapolis, MN, USA). The kits for detecting TG (#A110-1-1), non-esterified fatty acids (NEFA) (#A042-2-1), superoxide dismutase (SOD) (#A001-3-2), catalase (CAT) (#A007-1-1), and malondialdehyde (MDA) (#A003-1-2) were all obtained from Nanjing Jiancheng Bioengineering Institute (Nanjing, China). The Mito-Tracker Red CMXRos dye was purchased from Beyotime Biotech (Shanghai, China). The β-actin (#4967), FASN (#3180), Caspase-1 (#2225), IL-1β (#12242), HSL (#4107), ATGL (#2138), and the horseradish peroxidase-conjugated secondary antibodies were purchased from Cell Signaling Technology (Danvers, MA, USA). The SREBP1c (#AF6283), IL-18 (#DF6252), ASC (#DF6304) antibodies, and the GDF15 antibody (#DF6006) for immunofluorescence staining were purchased from Affinity Biosciences (Cincinnati, OH, USA). The SCD-1 (#db4883) and CD36 (#db8636) antibodies were purchased from Diagbio (Hangzhou, Zhejiang, China). The AIM2 (#ab119791), PPARα (#ab24509), the goat anti-rabbit secondary antibody (#ab150077) for immunofluorescence staining, and the dichlorodihydrofluorescein diacetate (DCFH-DA) ROS assay kit (#ab113851) were purchased from Abcam (Cambridge, MA, USA). DNA and RNA extraction kits were obtained from Aidlab Biotech (Beijing, China). The iScript cDNA synthesis kit and SYBR master mix were purchased from Bio-Rad (Hercules, CA, USA). The bicinchoninic acid (BCA) assay kit was obtained from Pierce (Rockford, IL, USA). The Western Lightning™ Plus-ECL Enhanced chemiluminescence Substrate assay kit was purchased from PerkinElmer (Waltham, MA, USA). Low-fat diet (LFD) contains 10% calories from fat (#D12450J), and HFD contains 60% calories from fat (#D12492) were purchased from Research Diet (New Brunswick, NJ, USA).

2.2. Cell culture and treatment

The human hepatic HepG2 and Huh-7 cell lines were purchased from the American Type Culture Collection (ATCC, Rockville, MD, USA) and cultured in a complete medium (DMEM, 10% FBS, and 1% penicillin/streptomycin) and maintained in a 5% CO_2 incubator at 37 °C. To establish an *in vitro* model of hepatic steatosis, HepG2 and Huh-7 cells were treated with 1 mM FFA (OA and PA at a 2:1 vol ratio) in a complete medium containing 1% fatty acid-free bovine serum albumin (BSA) for 24 h. Control cells were treated with 1% fatty acid-free BSA. Cell viability was assessed by MTT assay as previously described [45]. Briefly, cells were seeded in 96-well plates at 3×10^4 cells/well and incubated until cells reach 50% confluence. Cells were then treated with 1 mM FFA for 24 h and then subjected to MTT assay.

2.3. Animal study

NAG-1/GDF15 transgenic mice were previously generated to ubiquitously express human NAG-1/GDF15 (hNAG-1/GDF15) using protamine Cre mice on a C57BL/6 background [46]. The animals were a

kind gift from Dr. Thomas Eling at the National Institute of Environmental Health Sciences (NIEHS). This study was approved by the Committee on the Ethics of Animal Experiments of Zhejiang Chinese Medical University (Permit Number: SYXK 2018–0012). All animal protocols were performed following the Guide for the Care and Use of Laboratory Animals of the National Institutes of Health and complied with the Animal Welfare Act Regulations. Male mice aged 10 weeks old were placed on LFD or HFD for 12 weeks to induce hepatic steatosis. Body weights were measured once a week. At necropsy, the mice were sacrificed with CO_2, and blood was collected via the cardiac puncture method. The serum was collected by centrifugation at 3000 rpm for 10 min at 4 °C after separation. Tissues were snap-frozen in liquid nitrogen or fixed in formalin for further analysis.

2.4. Histological analysis

Hematoxylin and eosin (H&E) staining was performed to observe lipid accumulation in liver tissue. Liver tissue was fixed in 10% neutral formalin and paraffin-embedded, sectioned and processed by standard H&E procedures.

2.5. Bioinformatic analysis of NAG-1/GDF15 and AIM2 expression from published data sets

The publicly available raw transcriptomic data were downloaded from the GEO database (http://www.ncbi.nlm.nih.gov/geo/). NAG-1/GDF15 expression was analyzed in the liver tissue of patients with NAFLD (GEO accession numbers: GSE48452, GSE89632, and GSE126848). The expressions of the components of the AIM2 inflammasome (AIM2, ASC, and Caspase-1) and inflammatory cytokine IL-1β and IL-18 in the liver tissue of HFD-fed mice and patients with NAFLD were analyzed using the GSE119441 and GSE46300 datasets, respectively. Heatmap was built using MultiExperiment Viewer (MeV 4.9.0) software.

2.6. Plasmid transfection

The pcDNA3.1-NAG-1/GDF15 plasmid was a kind gift from Dr. Thomas Eling at NIEHS, which has been previously described [47]. HepG2 and Huh-7 cells were seeded in 6-well plates at 2×10^5 cells/well and incubated until cells reached 60% confluence. A total of 1.5 μg of pcDNA3.1-NAG-1/GDF15 or pcDNA3.1-Con (empty vector for expression control) were transfected into cells using Lipofectamin® 2000 reagent according to the manufacturer's instruction. After 24 h transfection, the efficiency of transfection was confirmed using qRT-PCR and Western blotting analysis. To determine the role of NAG-1/GDF15 in hepatic steatosis, following plasmid transfection overnight, the medium was removed, and cells were washed with phosphate-buffered saline (PBS) and treated with 1 mM FFA for 24 h.

2.7. RNA interference

The small interfering RNAs (siRNA) targeting NAG-1/GDF15 were produced by RiboBio (Guangzhou, China), which has the following sequences: (sense): 5′-GCUCCAGACCUAUGAUGACUUTT-3'. Briefly, 2×10^5 cells/well HepG2 and Huh-7 cells were seeded in 6-well plates and grown to 60% confluence. Cells were transfected with 100 nM NAG-1/GDF15 siRNA or negative control siRNA using Lipofectamin® 2000 reagent for 24 h according to the manufacturer's instruction. The efficiency of NAG-1/GDF15 knockdown was confirmed using qRT-PCR and Western blotting analysis. Following siRNA transfection, cells were treated with 1 mM FFA for up to 24 h to evaluate the role of NAG-1/GDF15 in hepatic steatosis.

2.8. Oil Red O staining

Oil Red O working solution was prepared by mixing the stock solution with distilled water (3:2), followed by incubation for 20 min and further filtration through a 0.22 μm filter. HepG2 and Huh-7 cells (2×10^5 cells/well) were seeded in 6-well plates. Upon each treatment, cells were washed twice with PBS and fixed with 4% paraformaldehyde for 10 min at room temperature. Cells were stained with Oil Red O solution for 1 h. Dishes were then washed three times with distilled water, dried, and photographed. To quantify the amount of Oil Red O, stained cells were dissolved in isopropanol and the absorbance was measured by a multi-well plate reader at 520 nm.

2.9. Bodipy 493/503 fluorescence staining

For Bodipy staining, HepG2 and Huh-7 cells were plated onto the laser confocal culture dish (1×10^5 cells/well) and treated with 1 mM FFA for 24 h. The cells were washed twice with PBS and fixed with 4% paraformaldehyde for 10 min at room temperature. Cells were stained with 1 μM Bodipy 493/503 and then incubated at 37 °C for 1 h in the dark. The nucleus was stained with DAPI. Cells were then washed three times with PBS and photographed using a laser confocal microscope (LSM880, Carl Zeiss, Germany). ImageJ 1.4.1 software (Bethesda, MD, USA) was used to quantify the amount of fluorescence in cells.

2.10. Determination of intracellular TG content

To investigate the intracellular content of TG, HepG2 and Huh-7 cells were washed with PBS, harvested by trypsinization, and then resuspended in PBS. Subsequently, the cell suspension was homogenized by sonication for 5 min. Triglyceride content was determined using a commercial TG assay kit according to the manufacturer's protocol. The protein concentration was determined by the BCA protein assay kit, and then the intracellular content of TG was normalized to the total protein concentration in the cell lysates.

2.11. Immunofluorescence assay for NAG-1/GDF15 detection

An immunofluorescence assay was performed to examine the expression of NAG-1/GDF15 in HepG2 and Huh-7 cells. Briefly, cells were seeded in the laser confocal culture dish at a density of 1×10^5 cells/well. The cells were treated with 1 mM FFA for 24 h, and then were washed twice with PBS and fixed with 4% paraformaldehyde followed by a permeabilization step with 0.5% Triton X-100. Afterward, cells were blocked with 5% BSA for 1 h. The cells were then incubated with the NAG-1/GDF15 antibody (1:500) at 4 °C overnight and followed by incubation with the secondary antibody. The nucleus was stained with DAPI in the dark. Cells were then washed three times with PBS and photographed using the LSM880 laser confocal microscope. ImageJ software was used to quantify the amount of fluorescence.

2.12. Detection of intracellular ROS

Intracellular ROS generation was detected using DCFH-DA fluorescence probe. Briefly, HepG2 and Huh-7 cells were seeded in the laser confocal culture dish at a density of 1×10^5 cells/well. After FFA treatment for 24 h, cells were stained with DCFH-DA (10 μM) for 30 min in the dark at 37 °C. Cells were then washed three times with serum-free DMEM and the amount of ROS in cells were either detected using the LSM880 laser confocal microscope or the Guava EasyCyte flow cytometer (Merck KGaA, Darmstadt, Germany).

2.13. Measurement of intracellular double-stranded DNA release

To determine intracellular dsDNA release, cells were stained with PicoGreen, Mito-Tracker Red, and DAPI. Briefly, cells were stained by

diluting the stock PicoGreen solution at 3 μL/mL directly into the cell culture medium and then incubated at 37 °C for 1 h in the dark. Cells were washed three times with PBS and then co-stained with 100 nM Mito-Tracker Red for 20 min in the dark at 37 °C. Afterward, the cells were fixed with 4% paraformaldehyde for 10 min at room temperature. The nucleus was stained with DAPI in the dark. After washing with PBS, the cells were photographed using the LSM880 laser confocal microscope.

2.14. Biochemistry assay and ELISA analysis

The lipid contents in liver tissue were determined using commercial kits for TG and NEFA. The activities of SOD and CAT, and the level of MDA in liver tissue and HepG2 and Huh-7 cells were detected by commercial kits. Serum samples were collected at necropsy. The serum levels of NAG-1/GDF15, IL-1β, and IL-18 were measured using ELISA kits. The serum levels of TG, total cholesterol (TC), NEFA, low-density lipoprotein (LDL), and high-density lipoprotein (HDL), as well as serum alanine transaminase (ALT) and aspartate transaminase (AST) activities were measured by Hitachi 3100 automatic biochemical analyzer (Hitachi Ltd. Tokyo, Japan). The release of DNA into the serum and the medium were determined using the Quant-iT PicoGreen dsDNA assay kit. All of the above endpoints were measured according to the manufacturer's instructions accordingly.

2.15. Mitochondrial DNA copy number determination

Mitochondrial DNA (mtDNA) was quantified by real-time PCR using a CFX96 Real-time PCR system (Bio-Rad) and SYBR Green PCR master mix (Bio-Rad). Total DNA was extracted from liver tissue or HepG2 and Huh-7 cells using a DNA extraction kit according to the manufacturer's instruction. Total DNA (100 ng) was amplified using primers specific to D-loop (mitochondrial-encoded gene) and 18S rRNA (nuclear-encoded gene) genes (Supplementary Table S1). The PCR conditions were as follows: 95 °C for 10 min, followed by 40 cycles at 95 °C for 30 s, 60 °C for 30 s, and 72 °C for 30 s. The mtDNA copy number was calculated from the ratio of D-loop to 18S rRNA.

2.16. RNA exaction and quantitative real-time PCR analysis

Total RNA was extracted from liver tissue or HepG2 and Huh-7 cells by RNA extraction kit following the manufacturer's protocol. Total RNA (1 μg) was subjected to reverse transcribed to synthesize cDNA with an iScript cDNA synthesis kit following the manufacturer's protocol. Real-time PCR was performed to determine the expression of selected genes using the SYBR PCR master mix on the CFX96 Real-time PCR system. The sequences for the primers used in this study are listed in Supplementary Table S1. The PCR conditions consisted of 40 cycles, with 5 s denaturation at 95 °C, 30 s annealing at 60 °C, and 5 s extension at 65 °C. β-actin was used as the reference gene for all samples. Relative gene expression was calculated after normalization to β-actin following the $2^{-\Delta\Delta CT}$ method.

2.17. Western blotting analysis

Total protein from liver tissue or HepG2 and Huh-7 cells were extracted using standard methods and protein concentrations were determined by a BCA protein assay kit. A total of 40 μg of protein were loaded on SDS-PAGE gel and electrophoresed for 2 h at 100 V. Separated proteins were transferred to PVDF membrane at 100 V for 2 h on ice. Afterward, the membranes were blocked with 5% non-fat dry milk in Tris-buffered saline with Tween 20 (TBST) at room temperature for 1 h and incubated overnight at 4 °C with primary antibodies (1:1000 for all). The next day, the membranes were washed with TBST followed by a secondary antibody (1:2000) for 1 h. β-actin was used as the loading control. The signals were detected using the Minichemi™ 610 chemical imaging System (Beijing, China). ImageJ 1.41 software was used for the calculation of the optical density.

2.18. Statistical analysis

Data were expressed as the mean ± standard error (SE) from three independent experiments except for the animal feeding study. SPSS software 23 (SPSS Inc., Chicago, IL, USA) was used to carry out the statistical analysis. The difference between pairwise groups was examined for statistical significance by Student's t-test. One-way ANOVA was used for multiple comparisons followed by Bonferroni's post hoc test in HepG2 and Huh-7 cell models. The analysis of datasets containing comparisons with two variables from each mouse from the animal study was analyzed using two-way ANOVA, and the repeated measurements were corrected using the false discovery rate (FDR) approach of the Benjamini-Hochberg method with a q-value 0.05. Two-sided P-values were calculated, and a value of $P < 0.05$ was considered to be statistically significant.

3. Results

3.1. NAG-1/GDF15 is downregulated in hepatic steatosis patients and hepatocellular steatosis model

It has been reported that the circulating NAG-1/GDF15 level is elevated in NASH patients compared to the normal population and patients with fatty liver (steatosis) [32]. To determine whether NAG-1/GDF15 is deregulated during NAFLD pathogenesis, we first performed gene expression analysis of NAG-1/GDF15 in NAFLD patients using publicly available GEO datasets. Interestingly, the GEO data analysis revealed that the expression of NAG-1/GDF15 was significantly decreased in the liver tissues of patients with steatosis compared to normal subjects as analyzed from three datasets (Fig. 1A). However, there was no significant difference between NASH patients and normal subjects (Fig. 1A). In line with clinical data [32], hepatic NAG-1/GDF15 was significantly increased in pathologically more severe NASH patients than hepatic steatosis patients as analyzed from two datasets (GES48452 and GES89632, Fig. 1A).

We next tested whether NAG-1/GDF15 is also deregulated in an *in vitro* hepatic steatosis cellular model. We first optimized the working concentration of FFA. We found that 1 mM FFA had no cytotoxicity effects on HepG2 and Huh-7 cells as determined by the MTT assay (Supplementary Fig. S1), and this concentration was also used by many published studies [48,49]. To mimic the steatosis phenotype, HepG2 and Huh-7 cells were treated with 1 mM FFA for 24 h, which have been commonly used as an *in vitro* model of hepatic steatosis [50]. As expected, Oil Red O and Bodipy 493/503 staining showed that FFA treatment significantly induced lipid deposition inside HepG2 and Huh-7 cells (Fig. 1B–E). Furthermore, the levels of intracellular TG were significantly elevated in both cell lines upon FFA treatment (Fig. 1F). The expressions of the key molecules of hepatic lipogenesis and fatty acid uptake, including SREBP1c (precursor), FASN, SCD-1, and CD36 were remarkably increased in HepG2 and Huh-7 cells after FFA treatment as determined using qRT-PCR (Fig. 1G and H), which were further confirmed by Western blotting (Fig. 1I and Supplementary Figs. S2A and S2B). Next, the expression of NAG-1/GDF15 was determined. Consistent with what we found from GEO datasets, a remarkable reduction of NAG-1/GDF15 expressions at both the mRNA and protein levels was observed in FFA-treated HepG2 and Huh-7 cells (Fig. 1J and K). This result is supported by a recent study that found NAG-1/GDF15 expression was dramatically reduced at the protein level upon palmitic, oleic, or combined palmitic/oleic treatments in HepG2 cells [51]. Immunofluorescence assay further verified that NAG-1/GDF15 expression, which is located both in the nucleus and cytosol, was significantly decreased in FFA-treated HepG2 and Huh-7 cells (Fig. 1L, M). Taken together, these results indicate that hepatic NAG-1/GDF15 expression is

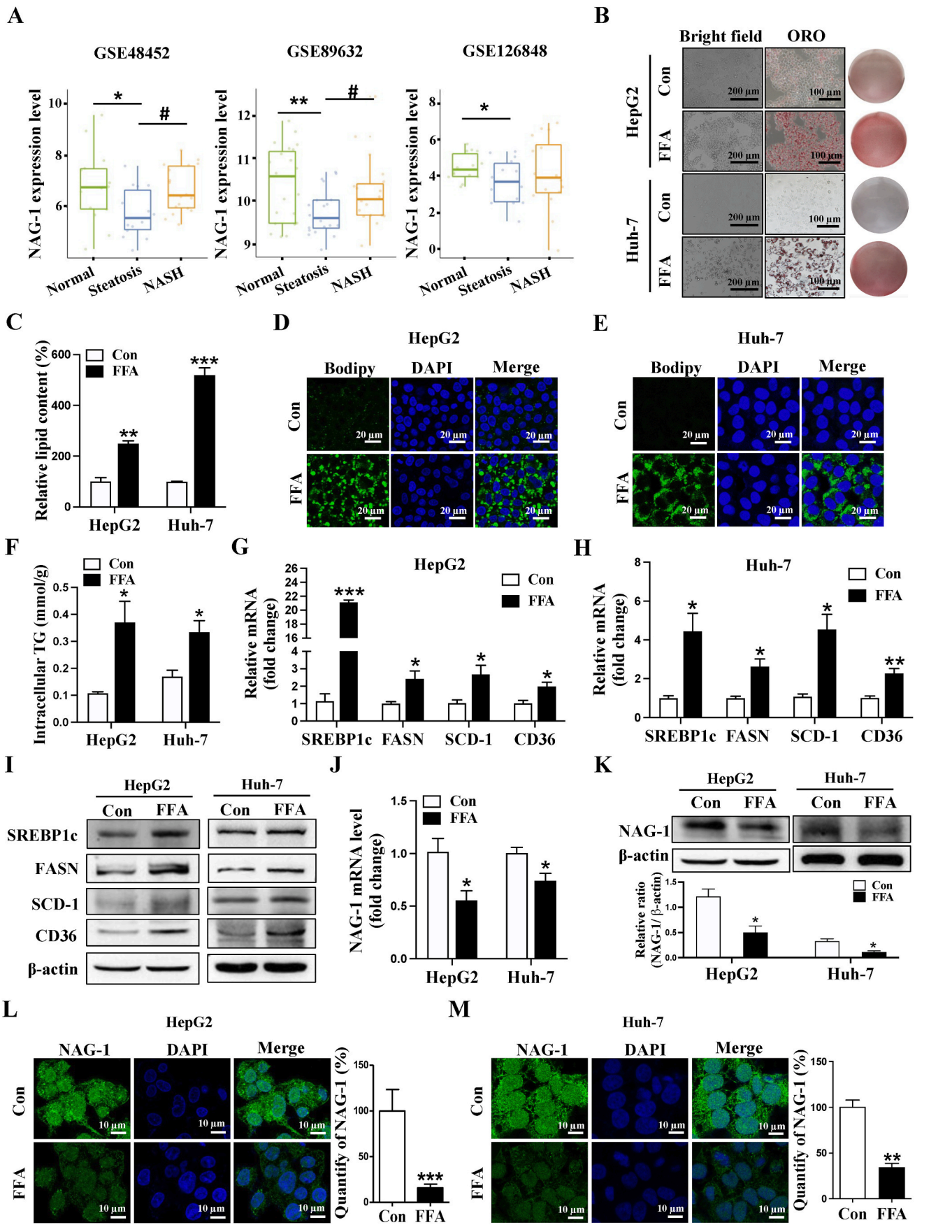

(caption on next page)

Fig. 1. NAG-1/GDF15 expression is decreased in hepatic steatosis patients and FFA-induced hepatocytes. (A) NAG-1/GDF15 mRNA expression in the liver of NAFLD and health patients from the GEO database. (B) Representative Oil Red O staining of lipid droplets accumulation after FFA treatment for 24 h in HepG2 and Huh-7 cells. Scale bar, 200 or 100 μm. (C) Quantitative analysis of Oil Red O staining. (D–E) Representative Bodipy 493/503 fluorescence staining of lipid droplets accumulation and quantitative analysis. Scale bar, 20 μm. (F) Intracellular TG content. (G–H) The expression of SREBP1c, FASN, SCD-1, CD36 at the mRNA level in HepG2 (G) and Huh-7 (H) cells as determined using qRT-PCR. (I) Western blotting analysis of the expression of SREBP1c, FASN, SCD-1, CD36 in HepG2 and Huh-7 cells. (J–K) The expression of NAG-1/GDF15 at the mRNA level (J) or protein level (K) in HepG2 and Huh-7 cells upon FFA treatment. The relative intensities of proteins were normalized against β-actin. (L–M) Representative immunofluorescence staining and quantification of NAG-1/GDF15 expression in HepG2 (L) and Huh-7 (M) cells. Data are shown as means ± SEM from three independent experiments, except for GEO analysis. Statistical analysis was performed using student's unpaired *t*-test (C-M, n = 3) or one-way ANOVA followed by Bonferroni's post hoc test (A, n = 14–23). $^{*}P < 0.05$, $^{**}P < 0.01$, $^{***}P < 0.001$ vs normal or control group; $^{\#}P < 0.05$ vs steatosis group. (For interpretation of the references to colour in this figure legend, the reader is referred to the Web version of this article.)

significantly reduced in the context of hepatic steatosis but may be elevated during the progression into the NASH stage.

3.2. Overexpression of NAG-1/GDF15 improves hepatic lipid metabolic disorders upon HFD

Next, we examined the effects of NAG-1/GDF15 on hepatic steatosis upon HFD treatment using a NAG-1/GDF15 Tg mouse model, which had a significantly high amount of circulating hNAG-1/GDF15 upon both diets (Fig. 2A). As shown in Fig. 2B, after feeding with HFD for 12 weeks, body weights were significantly increased in the WT mice compared with LFD (Fig. 2B). Consistent with what we have reported before [29], NAG-1/GDF15 overexpression significantly inhibited the increase of body weight in the Tg mice as compared to the WT mice upon HFD treatment (Fig. 2B). Under LFD, the body weight of the NAG-1/GDF15 Tg mice was also significantly lower than the WT mice. There were no significant changes in food intake (g/day/mouse) among all groups upon both diets as recorded for the continued 12 weeks (Supplementary Fig. S3A). Although at a non-significant level, mice on HFD seemed to eat less than mice on LFD (Supplementary Fig. S3A). The energy intake (kcal/day/mouse) was increased in HFD-fed mice compared with LFD-fed mice throughout the study period (Supplementary Fig. S3B). After adjusting for body mass, we found that NAG-1/GDF15 Tg mice had significantly increased energy intake (kcal/g/mouse) on both diets (Fig. 2C). We also found that NAG-1/GDF15 Tg mice significantly reduced HFD-induced hyperlipidemia and elevation in ALT and AST levels in the serum (Supplementary Fig. S4). Moreover, HFD significantly increased the weight of liver tissue and induced hepatic steatosis, while NAG-1/GDF15 overexpression significantly inhibited HFD-induced fat accumulation and steatosis in the liver of the C57BL/6 mice (Fig. 2D and E). Increased intrahepatic TG content and NEFA are serious risk factors for NAFLD and NASH [52]. We found that HFD markedly increased hepatic TG and NEFA levels in the WT mice, while these levels were significantly reduced in the NAG-1/GDF15 Tg mice (Fig. 2F).

We then examined the expression of the key molecules associated with hepatic lipogenesis and lipid uptake using qRT-PCR and Western blotting analysis. As shown in Fig. 2G, HFD significantly increased the mRNA expression of *SREBP1c*, *SCD-1*, and *CD36* in the liver tissues of the WT mice compared to LFD-fed WT mice. The expressions of these genes in the liver were markedly reduced in the NAG-1/GDF15 Tg mice upon both diets compared to the WT littermates (Fig. 2G). In addition, Western blotting analysis confirmed the above results (Fig. 2H). Interestingly, the expressions of FASN at both the mRNA and protein levels in the liver were significantly reduced upon HFD compared to LFD treatments in the WT mice as reported before [53] and were further reduced in the Tg mice on both diets (Fig. 2G and H).

Besides hepatic lipogenesis and fatty acid uptake, fatty acid β-oxidation and lipolysis are known as critical pathways that modulate lipid deposits in the liver [54,55]. Therefore, we examined the effects of NAG-1/GDF15 on the expression of genes associated with fatty acid β-oxidation and lipolysis. As shown in Fig. 3A–C, HFD significantly reduced the mRNA and protein expressions of the genes involved in fatty acid β-oxidation: (CPT1A, ACOX1, and PPARα); lipolysis: (ATGL and HSL) in the liver of the WT mice compared to LFD-fed WT mice. Interestingly, the expressions of the above molecules at both the mRNA and protein levels were significantly increased in the liver of the NAG-1/GDF15 Tg mice compared to the WT mice upon both diets (Fig. 3A–C). Taken together, these results suggest that NAG-1/GDF15 may prevent HFD-induced hepatic steatosis by regulating lipid metabolism including the inhibition of hepatic lipogenesis, decrease of fatty acid uptake, increase of β-oxidation, and enhancement of lipolysis in the liver.

3.3. NAG-1/GDF15 overexpression inhibits HFD-induced AIM2 inflammasome activation in mice

Inflammasome activation has been shown to play a critical role in conferring the pathogenesis of NAFLD [56]. However, very few studies have addressed the implication of AIM2 in hepatic steatosis, and whether AIM2 inflammasome participates in the anti-steatotic effects of NAG-1/GDF15 has not been reported. In our study, we first examined the gene expression profile of the AIM2 inflammasome components in HFD-fed mice (GSE119441) and patients with steatosis (GSE46300) using the GEO database. As shown in Fig. 4A, the levels of the AIM2 inflammasome family including *AIM2*, *ASC*, *caspase-1*, and *IL-1β* were increased in the liver of mice fed with HFD, which developed steatotic liver, compared to mice fed with the control diet. Similar to the above analysis, the expressions of the AIM2 inflammasome family were elevated in patients with steatosis than in the normal population (Supplementary Fig. S5). Due to the large inter-individual differences, only AIM2 or ASC were significantly increased in steatosis than the controls in the GSE119441 or the GSE46300 dataset, respectively (Fig. 4A, Fig. S5). Consistent with the results generated from the GEO database, the mRNA expression of *AIM2*, *ASC*, *caspase-1*, *IL-1β*, and *IL-18* were elevated in the liver of our WT mice upon HFD as determined using qRT-PCR (Fig. 4B). However, NAG-1/GDF15 overexpression significantly reduced the expression levels of these genes compared to WT mice upon HFD treatment (Fig. 4B). Most of the above results were further verified by Western blotting analysis (Fig. 4C). In addition, HFD significantly increased the serum level of IL-1β and IL-18 in the WT mice as determined using ELISA analysis, while these levels were both significantly reversed in the NAG-1/GDF15 Tg mice (Fig. 4D). Interestingly, the serum levels of IL-1β and IL-18 were both significantly lower in the NAG-1/GDF15 Tg mice compared to the WT littermates under LFD (Fig. 4D). Taken together, these data suggest that AIM2 inflammasome plays an important role in the pathogenesis of NAFLD in mice, while NAG-1/GDF15 can directly or indirectly inhibit AIM2 inflammasome activation and thereby prevent hepatic steatosis.

3.4. NAG-1/GDF15 protects against FFA-induced cellular steatosis in hepatocytes

To further investigate the role and underlying molecular mechanisms of NAG-1/GDF15 on hepatic steatosis, we examined the anti-steatosis effects of NAG-1/GDF15 in FFA-induced HepG2 and Huh-7 cells using genetic approaches. The expressions of NAG-1/GDF15 at both the mRNA and protein levels in HepG2 (Supplementary Figs. S6A and S6B) and Huh-7 (Supplementary Figs. S6C and S6D) cells were significantly increased upon pcDNA3.1-NAG-1/GDF15 plasmid

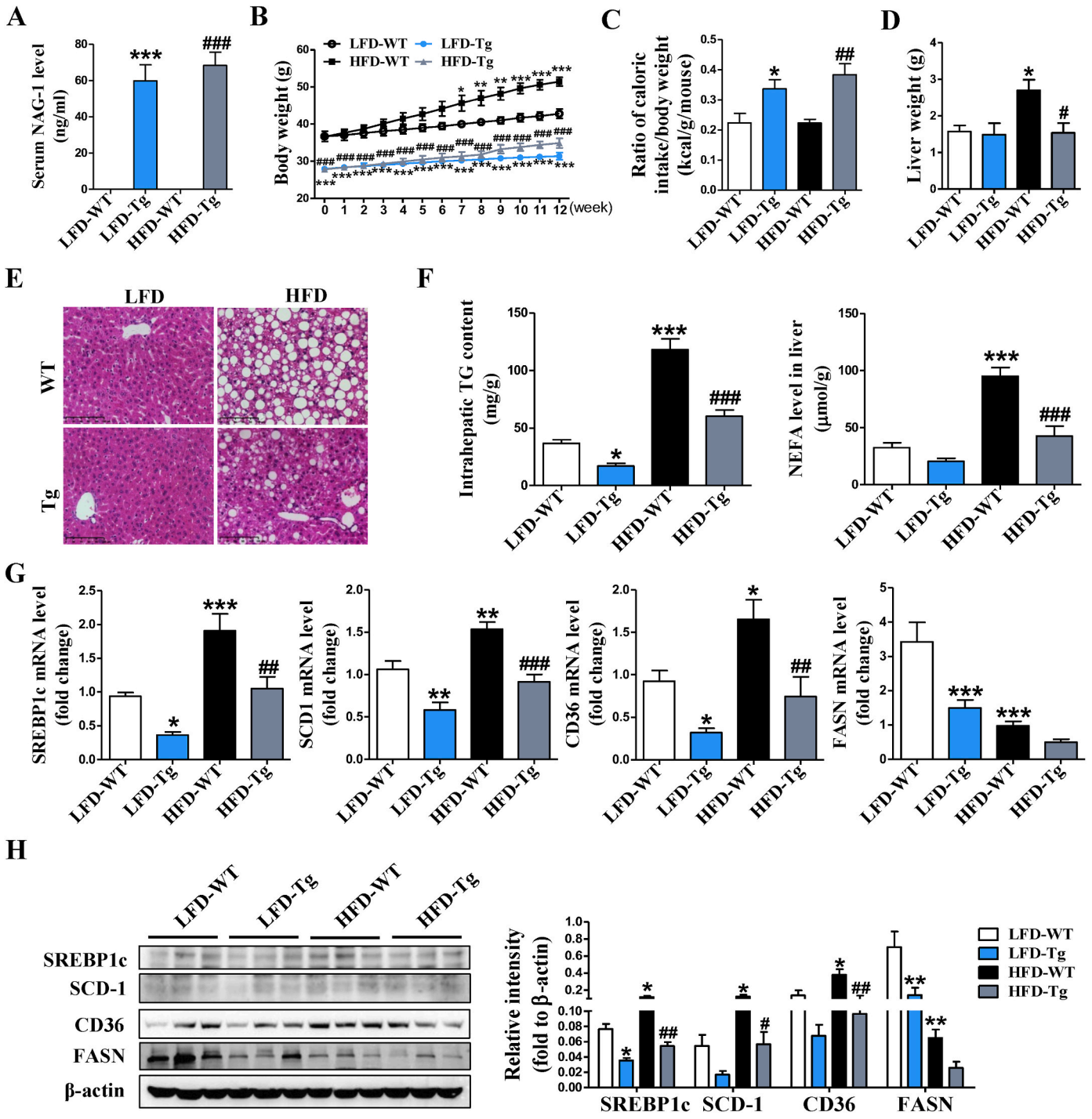

Fig. 2. NAG-1/GDF15 overexpression ameliorates HFD-induced hepatic steatosis and regulates lipid homeostasis in C57BL/6 mice. Mice were fed with LFD or HFD for 12 weeks. (A) Serum level of NAG-1/GDF15 as determined by ELISA. (B) Body weight changes. (C) Caloric intake adjusted for body weight. (D) Liver weight. (E) Representative H&E staining of liver tissues. Scale bar, 100 μm. (F) Hepatic TG and NEFA levels. (G–H) The expression of SREBP1c, SCD-1, CD36, and FASN at the mRNA level (G) or protein level (H) in the liver tissues as determined using qRT-PCR or Western blotting analysis. The relative intensities of proteins were normalized against β-actin. Data are shown as means ± SEM from three independent experiments, except for animal feeding study. Statistical analysis was performed using two-way ANOVA with post hoc Bonferroni's correction in B-D (n = 6 mice/group). Two-way ANOVA followed by the Benjamini-Hochberg method for the FDR correction was used for multiple measurements in A, F-G (n = 6 mice/group), and H (n = 3 mice/group). $^{*}P < 0.05$, $^{**}P < 0.01$, $^{***}P < 0.001$ vs WT LFD-fed mice, $^{\#}P < 0.05$, $^{\#\#}P < 0.01$, $^{\#\#\#}P < 0.001$ vs WT HFD-fed mice. FDR: false discovery rate.

transfection, while the basal expression of NAG-1/GDF15 was significantly reduced upon NAG-1/GDF15 siRNA treatment. As expected, NAG-1/GDF15 overexpression significantly diminished the lipid droplet accumulation in these hepatocytes that were treated with FFA compared to the control vector upon Oil Red O staining (Fig. 5A–C). There was a remarkable decrease in the intracellular TG level in the NAG-1/GDF15 overexpressing cells compared with FFA-treated control cells (Fig. 5D). On the contrary, knockdown of NAG-1/GDF15 significantly increased cellular lipid accumulation compared to scrambled siRNA (siRNA-Con) (Fig. 5E–G). Similarly, the intracellular TG level was

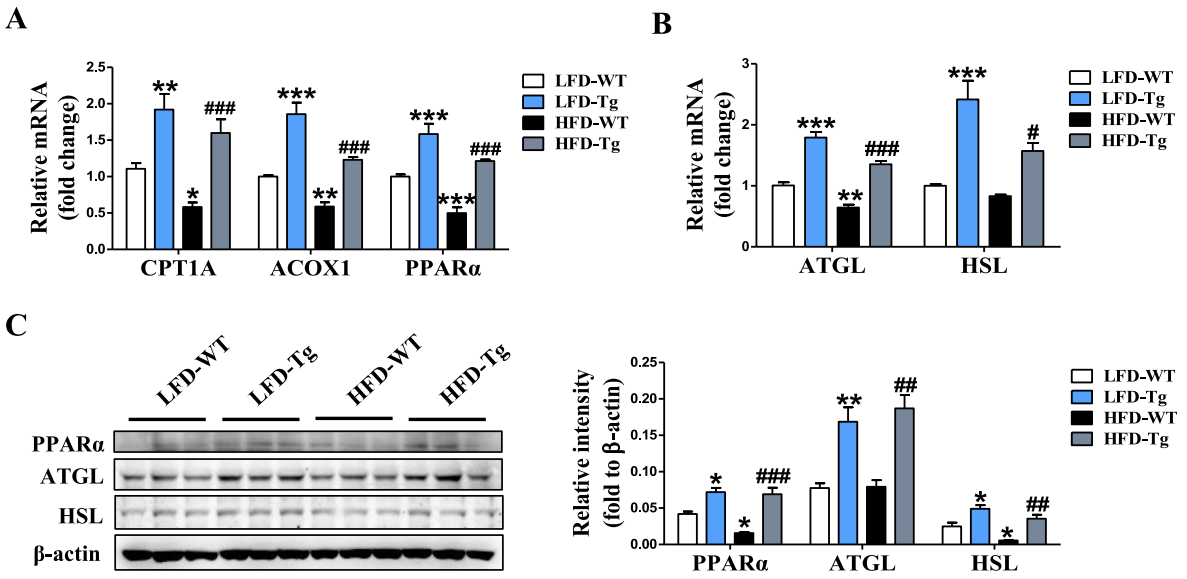

Fig. 3. NAG-1/GDF15 overexpression increases the expressions of the key genes and protein related to β-oxidation and lipolysis in mice upon both diets. Mice were fed with LFD or HFD for 12 weeks. (A–B) Expression of the key genes related to β-oxidation (A) and lipolysis (B) at the mRNA level in the liver tissues as determined using qRT-PCR. (C) Western blotting and densitometry analysis of the expressions of PPARα, HSL, and ATGL in liver tissues. The relative intensities of proteins were normalized against β-actin. Data are shown as means ± SEM from three independent experiments. Statistical analysis was performed using two-way ANOVA followed by the Benjamini-Hochberg method for the FDR correction in Figure A–B (n = 6 mice/group), and C (n = 3 mice/group). $^{*}P < 0.05$, $^{**}P < 0.01$, $^{***}P < 0.001$ vs WT LFD-fed mice, $^{\#}P < 0.05$, $^{\#\#}P < 0.01$, $^{\#\#\#}P < 0.001$ vs WT HFD-fed mice.

significantly increased in NAG-1/GDF15 knockdown cells compared to the control cells upon FFA treatment (Fig. 5H). Furthermore, Bodipy 493/503 staining revealed that the lipid droplets accumulation was significantly reduced in NAG-1/GDF15 overexpressing cells upon FFA treatment (Fig. 5I and J). In contrast, knocking down NAG-1/GDF15 profoundly further increased lipid droplet accumulation in HepG2 cells (Fig. 5K) and Huh-7 cells (Fig. 5L) upon FFA treatment. Collectively, these data suggest that NAG-1/GDF15 is critical in protecting against FFA-induced lipid accumulation in the hepatocellular steatosis model.

3.5. NAG-1/GDF15 inhibits hepatic steatosis via improving lipid metabolism dysregulation in hepatocytes

To determine whether lipid metabolism is involved in the anti-steatotic effect of NAG-1/GDF15 in hepatocytes, we next examined the expressions of the key molecules of hepatic lipogenesis and lipid uptake in HepG2 and Huh-7 cells using both qRT-PCR and Western blotting analysis. As shown in Fig. 6A and B, NAG-1/GDF15 overexpression significantly inhibited FFA-induced upregulation of the expressions of SREBP1c, FASN, SCD-1, and CD36 at both the mRNA and protein levels compared to the negative control in FFA-treated HepG2 and Huh-7 cells. In contrast, knockdown of NAG-1/GDF15 further increased FFA-induced upregulation of the expressions of these genes compared to the negative control (Fig. 6C and D). Supplementary Figs. S7A and S7B show densitometric analysis of western blots.

Furthermore, we examined the effects of NAG-1/GDF15 on fatty acid β-oxidation and lipolysis in FFA-induced hepatocytes. We found that overexpression of NAG-1/GDF15 significantly reversed FFA-induced downregulation of the expressions of *CPT1A*, *ACOX1*, *PPARα*, *ATGL*, and *HSL* at the mRNA level in FFA-induced HepG2 and Huh-7 cells (Fig. 6E). In contrast, NAG-1/GDF15 knockdown profoundly downregulated the expressions of these genes at the mRNA level compared to the negative control in HepG2 and Huh-7 cells upon FFA treatment (Fig. 6G). Western blotting further confirmed that the expressions of these molecules at the protein level were similar to their expression at the mRNA level (Fig. 6F, H). Supplementary Figs. S7C and S7D show densitometric analysis of western blots. Collectively, these data suggest that NAG-1/GDF15 may inhibit hepatic steatosis by regulating lipid metabolism in the aspects of inhibiting lipid synthesis and uptake, increasing fatty acid β-oxidation, and promoting lipolysis in hepatocytes.

3.6. NAG-1/GDF15 suppresses AIM2 inflammasome activation in FFA-induced hepatocellular steatosis model

Consistent with our findings in HFD-fed mice, we found that the relative gene expressions of the components of the AIM2 inflammasome, including *AIM2*, *ASC*, *caspase-1*, *IL-1β*, and *IL-18*, were elevated in FFA-induced HepG2 and Huh-7 cells (Fig. 7A). In addition, the components of the AIM2 inflammasome were expressed at a similar pattern at the protein level as they were expressed at the mRNA level (Fig. 7B and Supplementary Fig. S7E). These data suggest that cellular steatosis is also associated with AIM2 inflammasome activation in hepatocytes upon FFA stimulation.

Next, we examined whether NAG-1/GDF15 is necessary for inhibiting the activation of AIM2 inflammasome in FFA-induced hepatocytes. As shown in Fig. 7C and D, NAG-1/GDF15 overexpression significantly inhibited the expression of AIM2 inflammasome components compared to the negative control in FFA-induced HepG2 and Huh-7 cells as determined using qRT-PCR or Western blotting. In contrast, there was a significantly further increased expression of the AIM2 inflammasome components observed in FFA-induced HepG2 and Huh-7 cells where NAG-1/GDF15 was knocked down (Fig. 7E and F). Supplementary Figs. S7F and S7G show densitometric analysis of western blots. Taken together, these data suggest that the inhibitory effect of NAG-1/GDF15 on hepatic steatosis is related to the inhibition of AIM2 inflammasome activation in hepatocytes.

3.7. NAG-1/GDF15 attenuates oxidative stress and ROS generation in FFA- or HFD-induced hepatic steatosis

Studies have demonstrated that ROS contributes to inflammasome activation and plays an important role in the development of NAFLD [57,58]. We next examined whether the inhibitory effect of NAG-1/GDF15 on AIM2 inflammasome activation is related to the

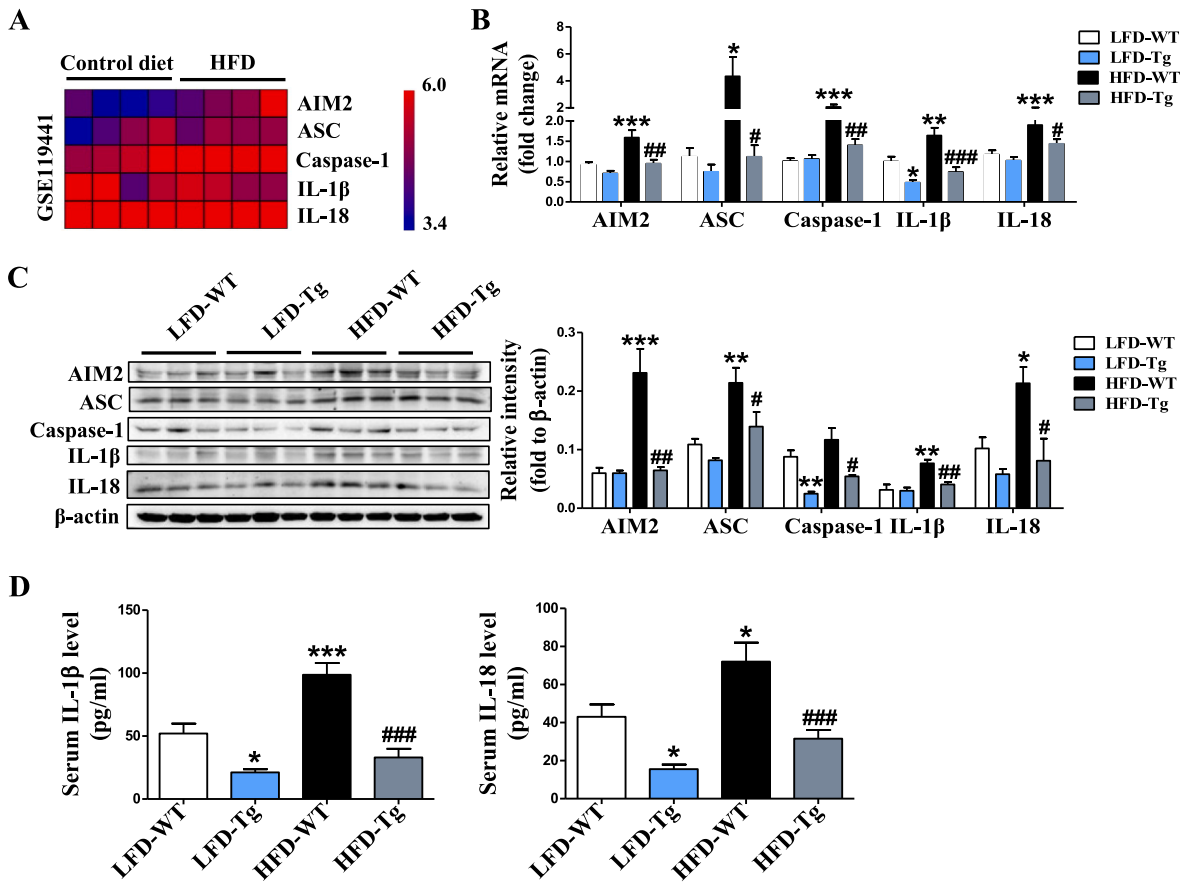

Fig. 4. NAG-1/GDF15 overexpression inhibits HFD-induced AIM2 inflammasome activation in mice. (A) Heatmap indicating differential mRNA expression of the components of AIM2 inflammasome (AIM2, ASC, Caspase-1, IL-1β, and IL-18) in liver tissues upon HFD treatment from the GEO database GSE119441. (B–C) The expression of AIM2 inflammasome components (AIM2, ASC, Caspase-1, IL-1β, and IL-18) at the mRNA level (B) and protein level (C) in the liver of the WT and NAG-1 Tg mice upon LFD and HFD as determined using qRT-PCR or Western blotting analysis. The relative intensities of proteins were normalized against β-actin. (D) Serum levels of IL-1β and IL-18 in mice upon both diets. Data are shown as means ± SEM from three independent experiments. Statistical analysis was performed using two-way ANOVA followed by the Benjamini-Hochberg method for the FDR correction in B and D (n = 6 mice/group), and C (n = 3 mice/group). $^{*}P < 0.05$, $^{**}P < 0.01$, $^{***}P < 0.001$ vs WT LFD-fed mice, $^{\#}P < 0.05$, $^{\#\#}P < 0.01$, $^{\#\#\#}P < 0.001$ vs WT HFD-fed mice.

regulation of ROS production in hepatic steatosis. Consistent with the previous report [59], we found that FFA treatment together with either Con-Vector (Fig. 8A, C) or siRNA-Con vector (Fig. 8B, D) significantly increased intracellular ROS generation in HepG2 cells as determined by DCFH-DA staining and flow cytometry analysis. However, NAG-1/GDF15 overexpression significantly reduced ROS production compared to the negative control in HepG2 cells upon FFA treatment (Fig. 8A, C). In contrast, knockdown of NAG-1/GDF15 further increased FFA-induced ROS generation compared to the negative control (Fig. 8B, D). Similar results were obtained in Huh-7 cells (Supplementary Figs. S8A and S8B).

SOD and CAT are the key antioxidant enzymes, which play crucial roles in maintaining the redox balance. To further investigate the effect of NAG-1/GDF15 on the status of oxidative stress, we examined the activities of SOD and CAT in HepG2 and Huh-7 cells. As shown in Fig. 8E and F, both SOD and CAT activities were significantly reduced upon FFA treatment, while NAG-1/GDF15 overexpression significantly reversed FFA-induced reduction of the enzymatic activities of SOD and CAT in HepG2 cells (Fig. 8E). In contrast, knockdown of NAG-1/GDF15 further decreased FFA-induced downregulation of the activities of these enzymes compared to the negative control (Fig. 8F). In addition, MDA, another indicator of oxidative stress whose level correlates with the level of intracellular ROS, was significantly increased upon FFA treatments (Fig. 8G and H). NAG-1/GDF15 overexpression significantly reversed the FFA-induced increase of MDA level in HepG2 cells (Fig. 8G), whereas NAG-1/GDF15 knockdown further increased MDA level compared to the negative control in FFA-treated cells (Fig. 8H). We further verified that the activities of SOD and CAT, and the level of MDA in Huh-7 cells were similar to that of the HepG2 cells (Supplementary Figs. S8C–F).

Furthermore, we measured the activities of SOD and CAT, and level of MDA in the liver of the HFD-fed mice. Similar to *in vitro* results, we found that HFD significantly reduced the activities of SOD and CAT, but increased MDA level in the liver of the WT mice, whose levels were all reversed in the NAG-1/GDF15 Tg mice upon HFD treatment (Supplementary Fig. S8G). NAG-1/GDF15 Tg mice also had significantly lower CAT levels than their WT littermates upon LFD (Supplementary Fig. S8G). Unfortunately, we could not measure ROS levels in the liver tissue due to technique difficulty. Collectively, these data suggest that NAG-1/GDF15 may prevent hepatic steatosis by suppressing AIM2 inflammasome activation mediated by reduced oxidative stress and ROS generation.

3.8. NAG-1/GDF15 inhibits dsDNA release from the mitochondria to cytosol in FFA- or HFD-induced hepatic steatosis

It has been previously reported that ROS overproduction causes mitochondrial damage and dysfunction which results in dsDNA leaking into the cytosol, thus triggering inflammasome activation during liver damage such as NAFLD [60,61]. In the present study, we found a significant reduction in the copy number of mtDNA in FFA-treated HepG2 cells, indicating that mitochondrial damage was induced (Fig. 9A). Interestingly, this reduction was significantly attenuated in the

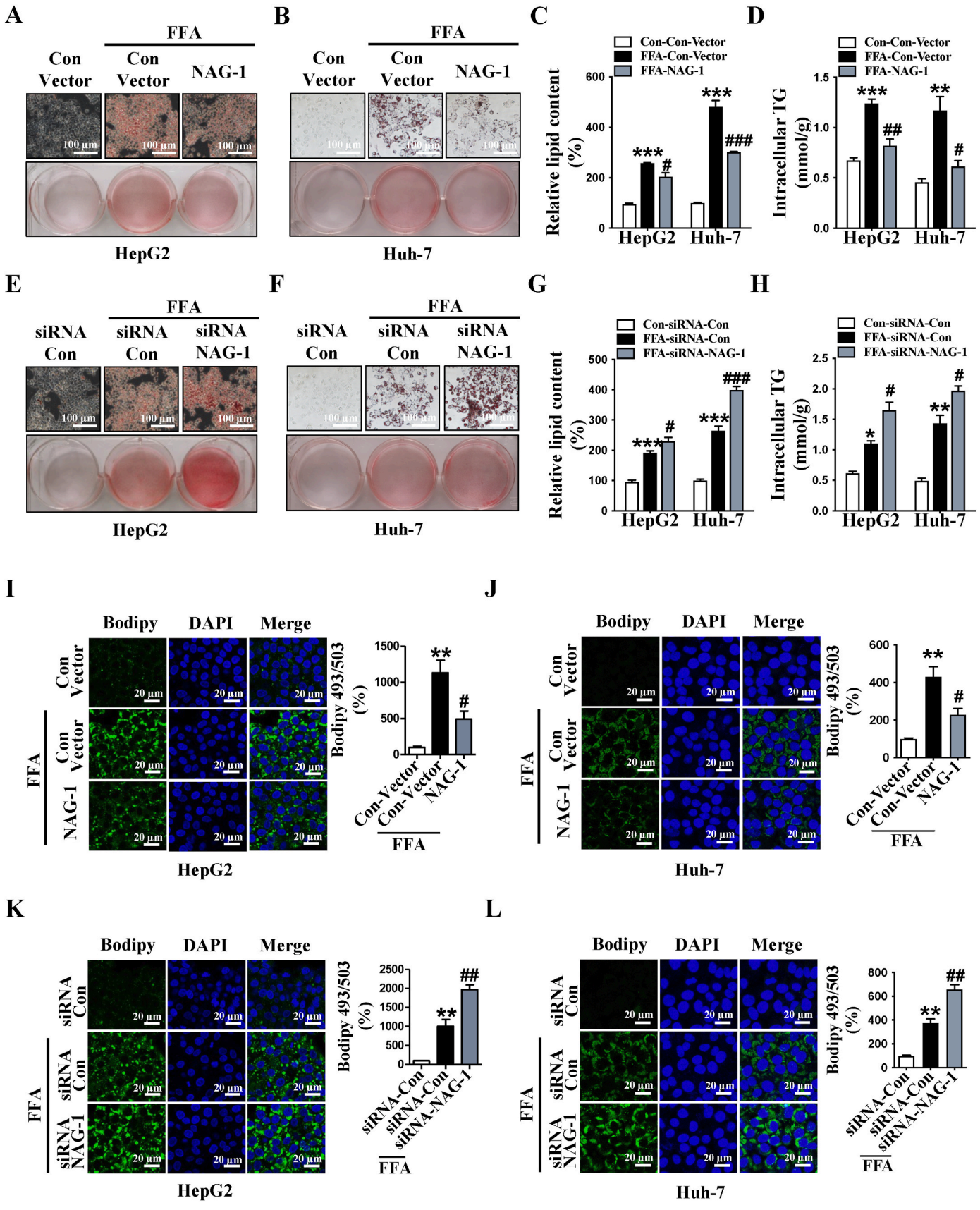

(caption on next page)

Fig. 5. NAG-1/GDF15 inhibits hepatic steatosis in the FFA-induced hepatocellular steatosis model. (A–B) Representative Oil Red O staining of lipid droplets accumulation in HepG2 (A) and Huh-7 (B) cells as transfected with pcDNA3.1-NAG-1 plasmid with or without FFA treatment. Scale bar, 100 μm. (C) Quantitative analysis of Oil Red O staining in HepG2 and Huh-7 cells as transfected with pcDNA3.1-NAG-1 plasmid with or without FFA treatment. (D) Intracellular TG content in HepG2 and Huh-7 cells as transfected with pcDNA3.1-NAG-1 plasmid. (E–F) Representative Oil Red O staining of lipid droplets accumulation in HepG2 (E) and Huh-7 (F) cells as transfected with NAG-1 siRNA with or without FFA treatment. Scale bar, 100 μm. (G) Quantitative analysis of Oil Red O staining in HepG2 and Huh-7 cells as transfected with NAG-1 siRNA with or without FFA treatment. (H) Intracellular TG content in HepG2 and Huh-7 cells as transfected with NAG-1 siRNA. (I–L) Representative Bodipy 493/503 fluorescence staining of lipid droplets accumulation and quantitative analysis in HepG2 cells as transfected with pcDNA3.1-NAG-1 plasmid (I) or NAG-1 siRNA (K) and in Huh-7 cells as transfected with pcDNA3.1-NAG-1 plasmid (J) or NAG-1 siRNA (L) with or without FFA treatment. Scale bar, 20 μm. Data are shown as means ± SEM from three independent experiments. Statistical analysis was performed using one-way ANOVA followed by Bonferroni's post hoc test (n = 3). $^{*}P < 0.05$, $^{**}P < 0.01$, $^{***}P < 0.001$ vs empty vector or negative control of siRNA, without FFA treatment, $^{\#}P < 0.05$, $^{\#\#}P < 0.01$ $^{\#\#\#}P < 0.001$ vs empty vector or negative control of siRNA, with FFA treatment. (For interpretation of the references to colour in this figure legend, the reader is referred to the Web version of this article.)

NAG-1/GDF15 overexpressing cells compared with FFA-treated control cells (Fig. 9A). In contrast, knockdown of NAG-1/GDF15 further decreased mtDNA copy number compared to the negative control in FFA-treated HepG2 cells (Fig. 9A). Similar results were observed in Huh-7 cells (Supplementary Fig. S9A). These data suggest that NAG-1/GDF15 could protect hepatic cells from FFA-induced mitochondrial damage.

Next, we used PicoGreen (dsDNA staining), Mito-tracker (specific for mitochondrial staining), and DAPI (nuclear staining) to examine mtDNA (dsDNA that co-localized with mitochondria), nuclear DNA (dsDNA that co-localized with nucleus), and cytosolic DNA (dsDNA that released into cytosol neither co-localize with mitochondria nor with the nucleus). As shown in Fig. 9B, FFA treatment significantly induced the release of dsDNA from mitochondria to the cytoplasm in HepG2 cells (as shown by the arrow, Fig. 9B (i), (iii)), whereas cytosolic DNA was barely detectable in untreated HepG2 cells (Con-Vector and siRNA-Con). However, NAG-1/GDF15 overexpression significantly inhibited FFA-induced dsDNA release compared to the negative control in FFA-treated HepG2 cells (as shown by arrow, Fig. 9B (ii)). In contrast, knockdown of NAG-1/GDF15 further increased FFA-induced dsDNA release compared to the negative control (as shown by arrow, Fig. 9B (iv)). Determination of the content of dsDNA in the medium further confirmed that FFA treatment significantly induced dsDNA release into the cytosol, while NAG-1/GDF15 inhibited dsDNA to leak into the cytosol (Fig. 9C). Similarly, we further verified that NAG-1/GDF15 also inhibited dsDNA release into the cytosol in Huh-7 cells (Supplementary Figs. S9B and S9C).

We further examined the copy number of hepatic mtDNA and the serum level of the released dsDNA in HFD-treated mice. Consistent with the previous report [62], HFD induced significant hepatic mitochondrial damage, which is evidenced by significantly reduced mtDNA copy number in the liver of the WT mice upon HFD (Supplementary Fig. S9D). In contrast, HFD-induced reduction of the copy number of hepatic mtDNA was significantly rescued in the NAG-1/GDF15 Tg mice (Supplementary Fig. S9D). Interestingly, the copy number of hepatic mtDNA was also profoundly higher in the NAG-1/GDF15 Tg mice than in the WT littermates under LFD (Supplementary Fig. S9D). Although at a non-significant level, the trend of the serum dsDNA level was similar to our results from the FFA-induced HepG2 and Huh-7 cellular steatosis cells (Supplementary Fig. S9E). Taken together, these results suggest that NAG-1/GDF15 could protect hepatic mitochondrial damage induced by FFA or HFD overload and thus inhibit ROS-induced dsDNA release into the cytosol, further inhibiting the activation of the AIM2 inflammasome, which in turn serves the mechanism of the inhibitory effect of NAG-1/GDF15 on hepatic steatosis.

4. Discussion

Growing evidence suggests that NAG-1/GDF15 is implicated in the pathogenesis of various metabolic disorders such as obesity, insulin resistance, myocardial infarction, atherosclerosis, and NAFLD [10,14]. Recently, both endogenous and exogenous NAG-1/GDF15 have been associated with the prevention of mice from steatosis and further development into NASH [33,34,36,63]. However, the exact molecular mechanisms underlying the protecting role of NAG-1/GDF15 in NAFLD remain elusive. In the present study, we identified NAG-1/GDF15 as a negative regulator of AIM2 inflammasome activation via inhibiting oxidative stress-mediated mitochondrial damage and dsDNA release, which results in the inhibition of the development of hepatic steatosis. Our *in vivo* study provides basic pathological insights into a potential correlation between AIM2 inflammasome and hepatic steatosis, which was downregulated by NAG-1/GDF15 overexpression in the Tg mice. Our *in vitro* results suggest that both ROS production and the expressions of the family members of the AIM2 inflammasome were increased in HepG2 and Huh-7 cells upon stimulation by FFA. NAG-1/GDF15 overexpression inhibited lipogenesis and rescued HepG2 and Huh-7 cells from FFA-induced cellular steatosis. On the contrary, knockdown of NAG-1/GDF15 increased lipogenesis and aggravated HepG2 and Huh-7 cells steatosis upon FFA treatment. Our study uncovered important mechanisms of NAG-1/GDF15 in the inhibition of hepatic steatosis through inhibiting ROS overproduction, mitochondrial damage, and dsDNA release into the cytosol, which results in inhibition of AIM2 activation and the secretion of inflammatory cytokines IL-18 and IL-β, and regulation of fatty acid homeostasis.

The liver plays a critical role in regulating lipid homeostasis which is responsible for orchestrating fatty acid synthesis, export, and subsequent redistribution to tissues [64]. SCD-1 and FASN are both key lipogenic enzymes in the *de novo* biogenesis of fatty acids, which were upregulated in patients with hepatic steatosis [65,66]. The inhibition of these two enzymes could reduce hepatic *de novo* lipogenesis and steatosis [67–69]. SREBP1c, a membrane-bound transcription factor, positively regulates lipogenic enzymes, including SCD-1 and FASN, and also plays a key role during hepatic steatosis and the development of NASH [70]. Knockdown of SREBP1c in the liver of ob/ob mice attenuated hepatic steatosis [71]. In addition, uptake of circulating fatty acids by the liver depends on their transmembrane transports, including the family of fatty acid transport proteins (FATPs) and the scavenger receptor CD36. CD36 expression is much lower in normal hepatocytes but is induced by the HFD diet, leading to TG accumulation and hepatic cell steatosis [72]. In contrast, disruption of CD36 expression could attenuate NAFLD [73].

Fatty acid β-oxidation and lipolysis are also important pathways that modulate hepatic lipid homeostasis [55]. Increasing mitochondrial respiratory activity in the liver could enhance the degradation of fatty acids and thus prevents their accumulation and the development of NAFLD [74]. However, the clinical implication of impaired mitochondrial β-oxidation on the progression of NAFLD is not conclusive, and contradicting reports have been published, both enhanced and decreased events have been reported [75–78]. PPARα is the most abundant PPAR isotype in the healthy liver, which regulates the expression of many β-oxidation-related genes, including CPT1 and ACOX1, and contributes to the remarkable metabolic flexibility of fatty acids in the liver [79–81]. PPARα is highly expressed in normal liver and decreased in NAFLD patients [82]. The deletion of either PPARα, CPT1 or ACOX1 in hepatocytes is sufficient to lead to aggravated NAFLD phenotypes [83–85]. The ATGL and HSL are key enzymes involved in TG

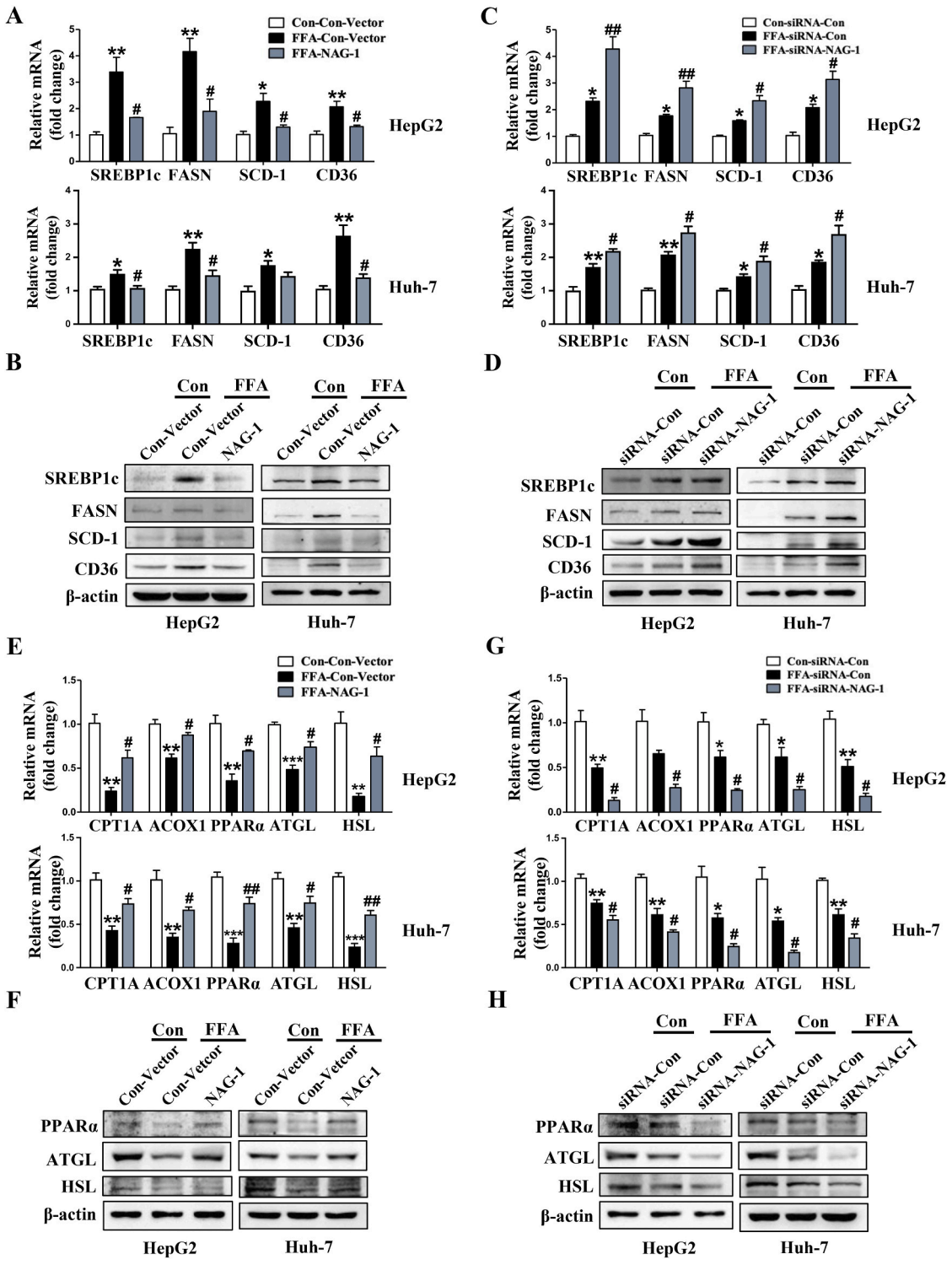

Fig. 6. NAG-1/GDF15 regulates lipid metabolism-related gene and protein expressions in the FFA-induced hepatocellular steatosis model. (A–B) Expression of lipogenesis- and lipid uptake-related molecules at the mRNA level (A) and protein level (B) in HepG2 and Huh-7 cells transfected with pcDNA3.1-NAG-1 plasmid as determined using qRT-PCR or Western blotting analysis. (C–D) Expression of lipogenesis- and lipid uptake-related molecules at the mRNA level (C) and protein level (D) in HepG2 and Huh-7 cells as transfected with NAG-1 siRNA. (E) Expression of the key genes related with fatty acid β oxidation and lipolysis at the mRNA level in HepG2 and Huh-7 cells as transfected with pcDNA3.1-NAG-1 plasmid. (F) Western blotting analysis of PPARα, ATGL, and HSL at the protein level in HepG2 and Huh-7 cells as transfected with pcDNA3.1-NAG-1 plasmid. (G) Expression of the key genes related with fatty acid β oxidation and lipolysis at the mRNA level in HepG2 and Huh-7 cells as transfected with NAG-1 siRNA. (H) Western blotting analysis of PPARα, ATGL, and HSL at the protein level in HepG2 and Huh-7 cells as transfected with NAG-1 siRNA. Data are shown as means ± SEM from three independent experiments. Statistical analysis was performed using one-way ANOVA followed by Bonferroni's post hoc test (n = 3). $^{*}P < 0.05$, $^{**}P < 0.01$, $^{***}P < 0.001$ vs empty vector or negative control of siRNA, without FFA treatment, $^{\#}P < 0.05$, $^{\#\#}P$ 0.01 vs empty vector or negative control of siRNA, with FFA treatment.

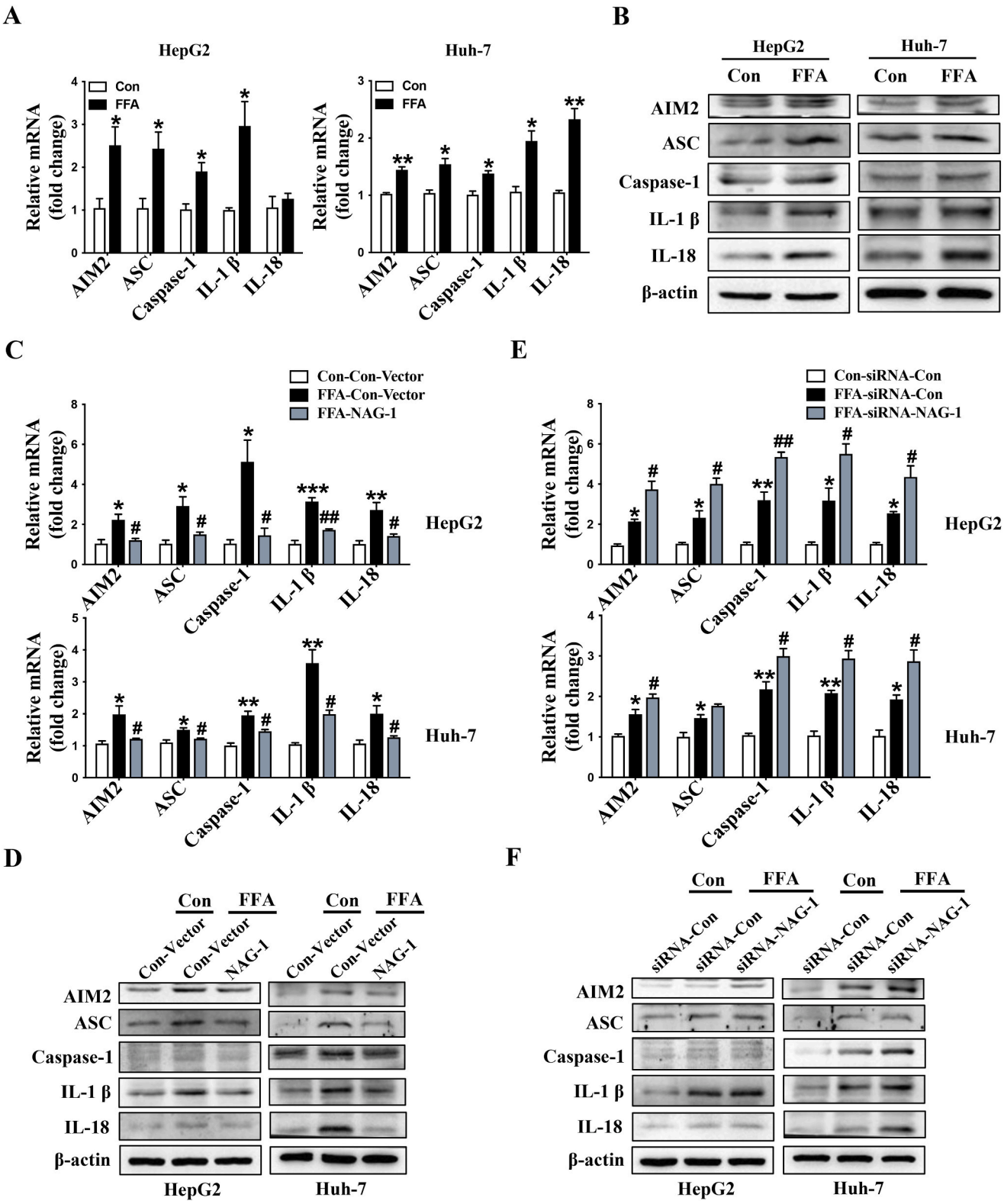

Fig. 7. NAG-1/GDF15 inhibits AIM2 inflammasome activation in the FFA-induced hepatocellular steatosis model. (A–B) The expression of AIM2 inflammasome (AIM2, ASC, Caspase-1, IL-1β, and IL-18) at the mRNA (A) and protein level (B) in HepG2 and Huh-7 cells upon treatment with FFA for 24 h as determined using qRT-PCR or Western blotting. (C–D) The mRNA (C) and protein (D) expression of AIM2 inflammasome components in HepG2 and Huh-7 cells as transfected with pcDNA3.1-NAG-1 plasmid with or without FFA treatment. (E, F) The expression of AIM2 inflammasome components at the mRNA (E) and protein level (F) in HepG2 and Huh-7 cells as transfected with NAG-1 siRNA with or without FFA treatment. Data are shown as means ± SEM from three independent experiments. Statistical analysis was performed using one-way ANOVA followed by Bonferroni's post hoc test (n = 3). $^{*}P < 0.05$, $^{**}P < 0.01$, $^{***}P < 0.001$ vs empty vector or negative control of siRNA, without FFA treatment, $^{\#}P < 0.05$, $^{\#\#}P < 0.01$ vs empty vector or negative control of siRNA, with FFA treatment.

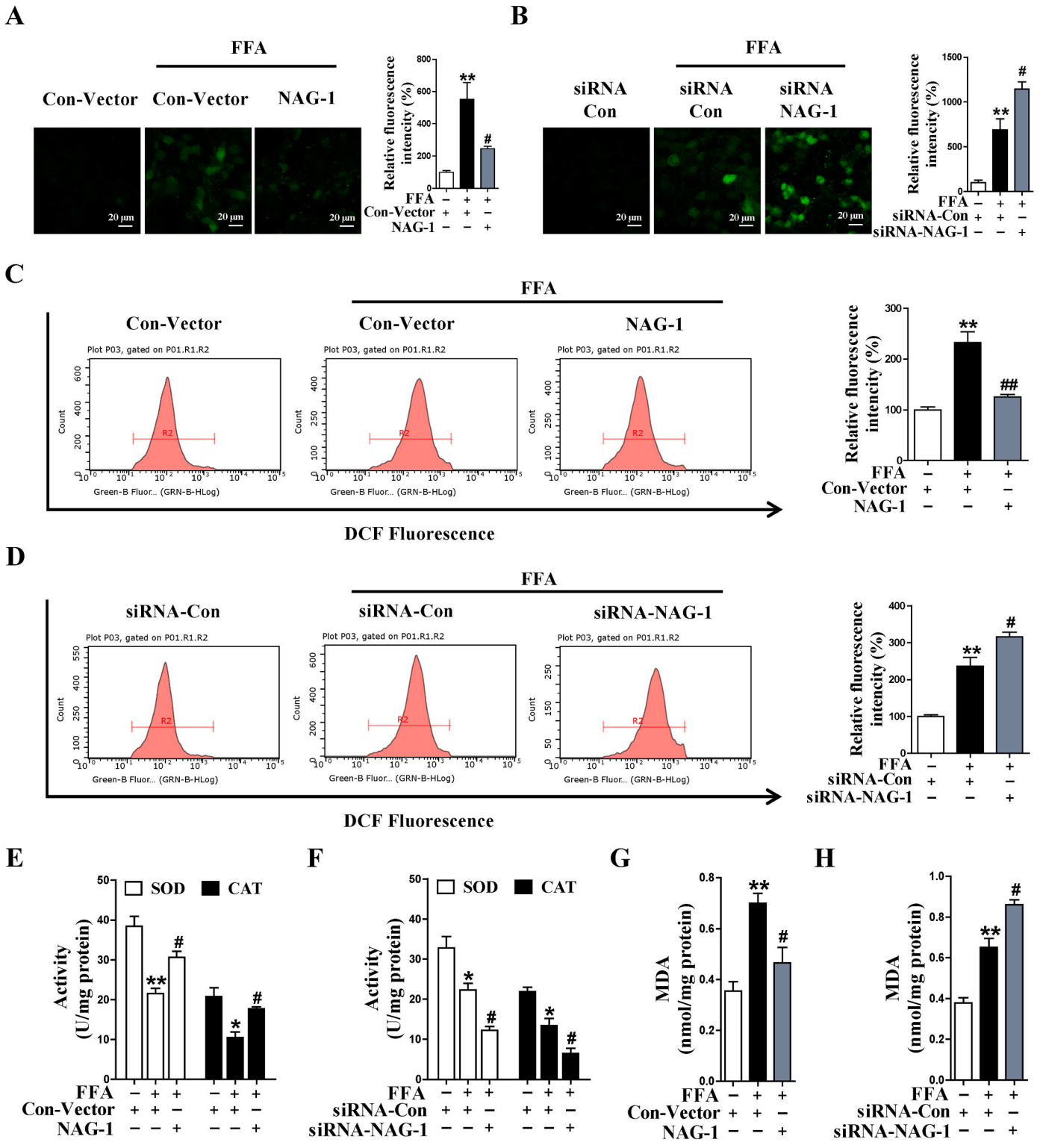

Fig. 8. NAG-1/GDF15 inhibits FFA-induced oxidative stress in HepG2 cells. (A–B) Representative DCFH-DA staining of intracellular ROS and quantitative analysis in HepG2 cells as transfected with pcDNA3.1-NAG-1 plasmid (A) or NAG-1 siRNA (B) with or without FFA treatment. Scale bar, 20 μm. (C–D) Intracellular ROS levels as determined using flow cytometry in HepG2 cells as transfected with pcDNA3.1-NAG-1 plasmid (C) or NAG-1 siRNA (D) with or without FFA treatment. (E–H) Hepatic activities of SOD and CAT, and level of MDA in HepG2 cells as transfected with pcDNA3.1-NAG-1 plasmid (E, G) or NAG-1 siRNA (F, H). Data are shown as means ± SEM from three independent experiments. Statistical analysis was performed using one-way ANOVA followed by Bonferroni's post hoc test (n = 3). $^{*}P < 0.05$, $^{**}P < 0.01$ vs empty vector or negative control of siRNA, without FFA treatment, $^{\#}P < 0.05$, $^{\#\#}P < 0.01$ vs empty vector or negative control of siRNA, with FFA treatment.

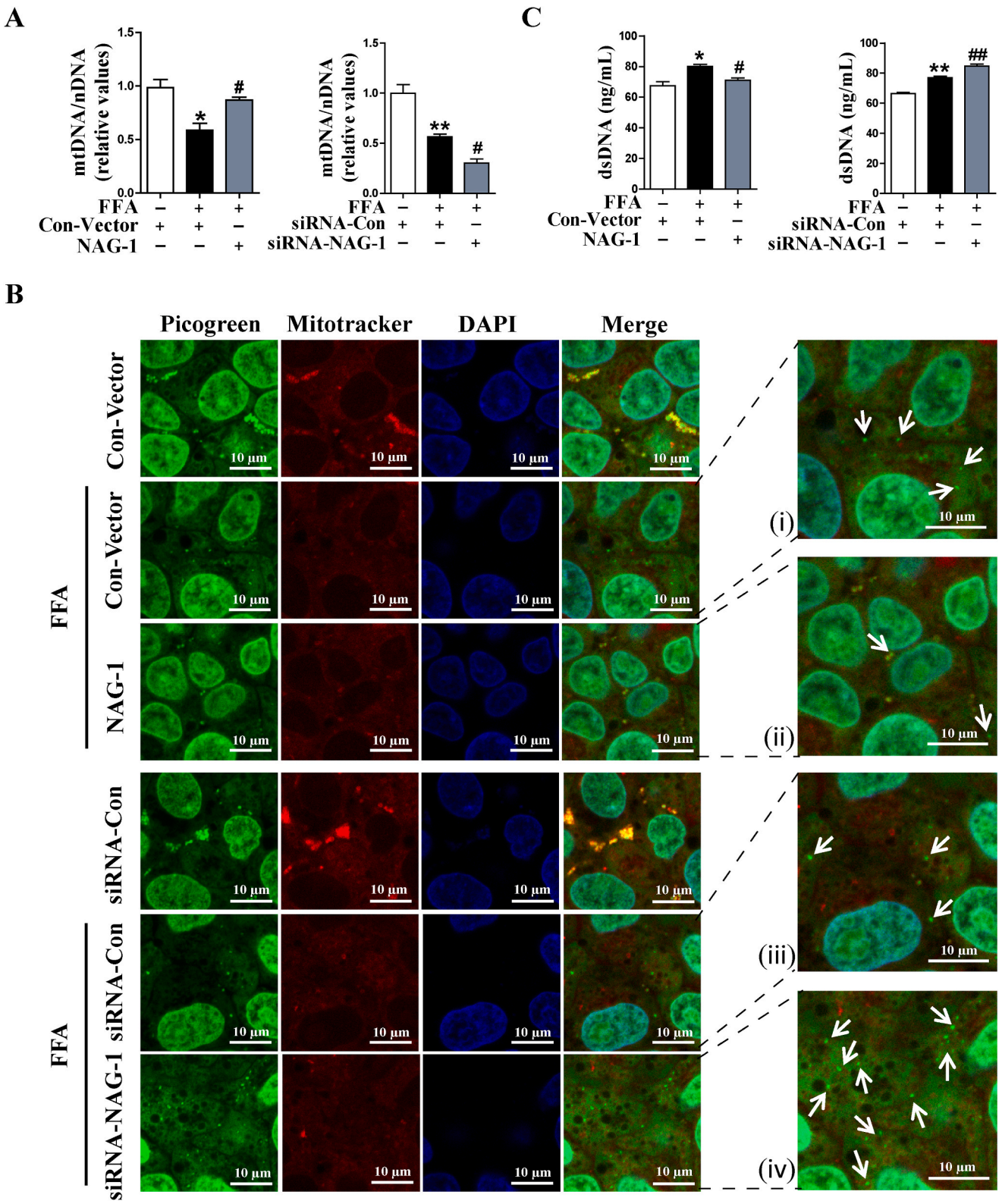

Fig. 9. NAG-1/GDF15 alleviates FFA-induced mitochondrial damage and suppresses FFA-induced mtDNA release from mitochondria in HepG2 cells. (A) The copy number of mtDNA as determined using qRT-PCR in HepG2 cells as transfected with pcDNA3.1-NAG-1 plasmid or NAG-1 siRNA with or without FFA treatment. (B) The release of dsDNA into the cytosol as determined using PicoGreen (dsDNA staining), Mito-tracker (mitochondrial staining), and DAPI (nuclear staining) in HepG2 cells as transfected with pcDNA3.1-NAG-1 plasmid or NAG-1 siRNA. Scale bar, 10 μm. White arrow points to cytosolic dsDNA (mtDNA release into the cytosol). (C) The content of dsDNA in the medium as determined using the PicoGreen fluorescent probe in HepG2 cells as transfected with pcDNA3.1-NAG-1 plasmid or NAG-1 siRNA. Data are shown as means ± SEM from three independent experiments. Statistical analysis was performed using one-way ANOVA followed by Bonferroni's post hoc test (n = 3). $^{*}P < 0.05$, $^{**}P < 0.01$ vs empty vector or negative control of siRNA, without FFA treatment, $^{\#}P < 0.05$, $^{\#\#}P < 0.01$ vs empty vector or negative control of siRNA, with FFA treatment.

decomposition, which have been associated with the development of NAFLD [64,86]. Liver-specific deletion of ATGL results in hepatic steatosis in mice [87], while hepatic overexpression of ATGL or HSL promoted fatty acid oxidation and ameliorated hepatic steatosis [88].

In line with the above evidence, our results showed that overexpression of NAG-1/GDF15 could downregulate the expression of fatty acid lipogenesis- and uptake-associated molecules, such as SREBP1c, FASN, SCD-1, and CD36 in both HFD and FFA-induced hepatic or cellular steatosis models. NAG-1/GDF15 also significantly increased the expression of the lipid decomposition-related key molecules, including ATGL, HSL, PPARa, CPT1, and ACOX1 in these models. In contrast, knockdown of NAG-1/GDF15 demonstrated opposite effects, indicating that NAG-1/GDF15 is critical in regulating lipid homeostasis and thus attenuating hepatic steatosis. Our previous study found that NAG-1/GDF15 overexpression alleviated HFD-induced obesity and insulin resistance in Tg mice via augmenting lipolysis, oxidative metabolism, and thermogenesis in adipose tissue [29]. Liver-specific deletion of NAG-1/GDF15 via adenovirus injection has been reported to increase hepatic lipid and TG accumulation, and to inhibit fatty acid β-oxidation in the liver of fasting mice, accompanied by reduced gene expression of PPARa, ACOX1, and CPT1a [35]. A recent study reported that overexpression of NAG-1/GDF15 through adenovirus transfection in mice or using recombinant protein in hepatic cells inhibited lipid accumulation and the progression of NASH [36]. Together with our study, the current evidence suggests that NAG-1/GDF15 could be a promising target for the prevention or treatment of steatosis and NAFLD-related metabolic deterioration via regulating fatty acids metabolism.

At present, whether NAG-1/GDF15 elicits its anti-obesity effect and thus inhibits the development of metabolic-related diseases exclusively through the anorexigenic effect or other mechanisms is still a debate. Contradictory results show the mechanisms underlying the anti-obesity effects of NAG-1/GDF15. Baek and Eling were the first to report the body weight-lowering effect of NAG-1/GDF15 in mice that ubiquitously overexpressing hNAG-1/GDF15 under the control of a chicken β-actin promoter [46]. Our previous study using the same mice showed that NAG-1/GDF15 overexpression decreased body weight and improved insulin resistance through increasing thermogenesis and energy expenditure, which was independent of food intake or energy intake adjusted for body mass [29]. Johnen et al. were the first that reported NAG-1/GDF15 may inhibit obesity by reducing appetite and food intake [30]. The anorexigenic mechanism was further supported by four studies demonstrating that exogenous NAG-1/GDF15 administration of recombinant hNAG-1/GDF15 leads to resistance to diet-induced obesity via glial cell line-derived neurotrophic factor (GDNF) family receptor alpha-like (GFRAL)-dependent anorexigenic action in mice [26–28,89]. However, results from several studies could not be solely explained by the anorexigenic action of NAG-1/GDF15 mediated via the GFRAL receptor [29,33,90–93].

For example, in ob/ob mice, administration of recombinant hNAG-1/GDF15 (Sigma) decreased body weight and improved insulin sensitivity without changing food intake or energy expenditure but may be attributed to elevated oxidative metabolism and lipid mobilization in the liver, muscle, and adipose tissues [90]. Overexpression of NAG-1/GDF15 via adenovirus injection resulted in significantly reduced liver weight, hepatic contents of TG, improved glucose tolerance, and NAFLD and liver damage in ob/ob mice, without difference in food intake, compared to control mice [35]. Kim et al. reported that hepatic-specific overexpression of hNAG-1/GDF15 inhibited steatosis and NASH development independent of food consumption [33]. In line with these studies, our previous [29] and current study suggest that the anti-obesity and the beneficial effects against NAFLD of NAG-1/GDF15 were not due to anorexigenic action. If food intake was calculated as calorie intake adjusted for body mass, our NAG-1/GDF15 Tg mice consumed significantly more food energy as compared to the WT mice. It is still not clear how exactly our NAG-1/GDF15 mice consumed more food energy than the WT mice. Our previous study suggests that NAG-1/GDF15 mice had increased thermogenesis, energy metabolism, and lipolysis [29], which may be a reason. As discussed before [94], these discrepancies in the effect of NAG-1/GDF15 on food consumption are probably attributed to differences in experimental methods, including genetic NAG-1/GDF15 overexpression vs. recombinant NAG-1/GDF15, a different source of recombinant NAG-1/GDF15, the concentration of circulating NAG-1/GDF15 in serum and tissues, duration of diet feeding or analytical methods of food intake measurement, etc. More studies are still needed to clarify whether the mechanisms underlying the anti-obesity effects of NAG-1/GDF15 are related to the anorexigenic effect.

Other than the GFRAL receptor, some studies suggest that the ALK5-TGFβRII complex also mediates the action of NAG-1/GDF15 in various tissues and cells [30,95]. Another study by Guillaume et al. reported that tamoxifen induced a rise in plasma concentration of NAG-1/GDF15 through a transcriptional mechanism dependent on hepatocyte estrogen receptor α (ERα) activation. The author found that ERα was associated with specific binding sites in the NAG-1/GDF15 regulatory region in hepatocytes upon tamoxifen treatment [96]. These studies suggest a possibility that NAG-1/GDF15 might exert its regulatory effects via receptors other than GFRAL or GFRAL independent mechanisms [97]. In our study, we did not detect the difference in GFRAL expression between the NAG-1/GDF15 Tg and WT mice in the hindbrain (data not shown). However, the expression of GRFAL has been reported in HepG2 cells [98]. Therefore, further studies are needed to elucidate whether GFRAL and/or other uncharacterized receptors are responsible for the beneficial effects of NAG-1/GDF15 in our mouse model.

At present, several studies have investigated the molecular mechanisms underlying the protective role of NAG-1/GDF15 against NAFLD. Similar to what we found in this study, NAG-1/GDF15 is likely to exert preventative and therapeutic effects against NAFLD via regulating lipid metabolism, such as inhibiting the fatty acid synthesis and enhancing fatty acid oxidation in the liver [33,35]. One interesting question is whether the anti-steatotic effect of NAG-1/GDF15 is simply a result of its inhibition of obesity. To exclude the weight-dependent effect, Kim et al. examined the protective effect of NAG-1/GDF15 during the pathogenesis of NAFLD by employing both an Amylin liver NASH (AMLN) diet and a methionine-choline deficient diet (MCDD) [33]. Both diets can induce hepatic steatosis and NASH in mice but exhibit distinctive effects on body weight in the mice [33]. The authors found that NAG-1/GDF15 may inhibit the progression of steatosis into NASH through its anti-inflammatory function in mice treated with both diets, which was independent of the anti-obesity effect of NAG-1/GDF15 [33].

Additionally, disruption of ER homeostasis (ER stress) due to unfolded protein accumulation and downstream signaling response has been proposed to play a crucial role in both the development of steatosis and progression to NASH [99]. The C/EBP-homologous protein (CHOP) has been shown to play a critical role in FFA-mediated ER stress-related liver cell death [100]. Several studies have demonstrated that CHOP alone or the PERK-activated CHOP signaling pathway could directly bind to the promoter of NAG-1/GDF15 under ER stress and transcriptionally upregulate NAG-1/GDF15 expression in different cell types [90,101–103]. Li et al. reported that NAG-1/GDF15 acted as a downstream component of CHOP, which is associated with reduced hepatic lipid accumulation and alleviated NAFLD progression in HFD-fed mice [104]. However, whether targeting ER redox homeostasis is a potential mechanism of NAG-1/GDF15 for its protective effects in hepatic steatosis in our model needs to be further examined.

Recently, NAG-1/GDF15 has been recognized to be a diagnostic marker for mitochondrial dysfunction and related diseases [13,105], suggesting that NAG-1/GDF15 also plays a role in respiratory chain dysfunction other than its general role in metabolic dysfunction. However, at present, no study has reported the regulatory effects of NAG-1/GDF15 on mitochondrial damage caused by the fatty acids overload and whether NAG-1/GDF15 could inhibit oxidative stress. In this study, we identified that AIM2 inflammasome inhibition by

NAG-1/GDF15 via reducing oxidative stress associated mitochondrial damage and dsDNA release may serve as a novel mechanism underlying the protective effect of NAG-1/GDF15 against NAFLD. We found that HFD or FFA-induced AIM2 inflammasome activation both in mouse livers or in HepG2 and Huh-7 cells, accompanied by mitochondrial damage, increased ROS and MDA levels, reduced SOD and CAT enzymatic activities in hepatocytes, and reduced dsDNA release into the cytosol. We also found that NAG-1/GDF15 overexpression in HFD-treated mice or FFA-treated hepatocytes significantly inhibited AIM2 inflammasome activation and alleviated mitochondrial damage-associated oxidative stress and dsDNA release. On the contrary, knockdown of NAG-1/GDF15 demonstrated opposite effects both *in vivo* and *in vitro*.

High serum FFA levels are associated with the pathogenesis of metabolic syndromes, such as NAFLD [106]. Previous studies reported that FFA can activate the NLRP3 inflammasome through ROS overproduction and dsDNA release upon mitochondrial damage [107]. Among all inflammasomes, NLRP3 is the most thoroughly studied inflammasome type, which is an important sensor of metabolic dysregulation and controls obesity-associated metabolic diseases, such as type 2 diabetes and NAFLD [108–110]. Stienstra et al. was the first to demonstrate that NLRP3, caspase-1, or ASC deletion inhibited obesity, improved insulin sensitivity, and inhibited hepatic steatosis in HFD-fed mice [111,112]. However, these results were challenged by Henao-Mejia et al. that deletion of NLRP3, caspase-1, IL-18, or IL-1β respectively, all developed exacerbated NASH compared to the WT mice under MCDD [113]. Nevertheless, most studies up to date suggest that NLRP3 activation promotes the development and progression of NAFLD, and deletion of the members of the NLRP3 family by genetic or pharmacological approaches prevented mice from developing steatosis, fibrosis, and/or NASH [114–118]. Our previous study also found that the expression of the components of the NLRP3 inflammasome is upregulated in the adipose tissue upon HFD in the WT mice but was reduced in our NAG-1/GDF15 Tg mice [119]. Unfortunately, in this study, there were no differences in the hepatic expression of NLRP3 at both the mRNA and protein levels between NAG-1/GDF15 Tg and WT mice under both diets (data not shown). Therefore, more studies are needed to clarify the discrepancies among studies.

AIM2 is another member of inflammasomes, which recognize dsDNA released during infection and is typically considered to be broadly involved in pathogen recognition [109], while the physiologic functions of AIM2 inflammasome remain obscure. The binding of DNA to AIM2 initiates the assembly of the AIM2 inflammasome complex, which results in ASC oligomerization and subsequent recruitment of pro-caspase-1 and leads to the release of inflammatory IL-18 and IL-1β [120]. Recently, studies have reported that AIM2 can also respond to dsDNA released from damaged host cells causing IL-18 and IL-1β secretion, thereby driving the development of sterile inflammatory diseases including neuronal disease, kidney disease, atherosclerosis, cardiovascular disease, insulin resistance, and diabetes, liver diseases, and cancer [121,122]. Increased expressions of AIM2, IL-1β, and circulating mtDNA were detected in patients with type 2 diabetes [123]. At present, several laboratory studies have examined the implication of AIM2 in the development of steatosis and NASH in mice, while human studies are still lacking [122]. AIM2 inflammasome has been found to be overexpressed and activated in the liver of the HFD-induced NAFLD mouse model [43,44]. Overexpress of the AIM2 gene in mice aggravated HFD-induced NAFLD and stimulated inflammatory cell infiltration and increased expression of inflammation-related genes (IL-1β and IL-18) [44]. In contrast, the knockdown of AIM2 led to alleviated NAFLD and the downregulation of IL-1β and IL-18 expressions [44]. Using MCDD-induced NAFLD/NASH mouse model, Csak et al. reported that steatosis and steatohepatitis were associated with both NLRP3 and AIM2 upregulation and activation [42]. The authors further found that AIM2 upregulation and activation were dependent on MyD88 in bone marrow (BM)-derived and non-BM-derived cells [42]. More studies are needed to further examine the molecular mechanism of AIM2 inflammasome activation during the development of NAFLD. Our study reported for the first time that the activation of the AIM2 inflammasome was inhibited by NAG-1/GDF15 through inhibiting oxidative stress and dsDNA release. However, further studies are needed to clarify the exact molecular mechanisms of how AIM2 inflammasome activation drives the development of hepatitis steatosis, and how NAG-1/GDF15 inhibits AIM2 inflammasome activation and thus inhibits obesity-related metabolic diseases.

There are a few limitations in this study. First, NAFLD encompasses simple steatosis to nonalcoholic steatohepatitis as well as further progression to cirrhosis and liver carcinoma. However, we did not examine the role of NAG-1/GDF15 in various stages of NAFLD, which needs to be further explored in future studies. In addition, emerging evidence has demonstrated that several signaling cascades, including TGF-β, mTOR, AMPK, Hedgehog signaling, MAPK, and NF-κB signaling all participate in the regulation of lipid metabolism in the liver, and pathogenesis of steatosis and NAFLD [124–126]. More studies are needed to determine the relationship between these signaling pathways and NAG-1/GDF15-induced AIM2 inactivation, and thus inhibit obesity-induced hepatic steatosis.

HFD is known to induce depletion of hepatic n-3 long-chain polyunsaturated fatty acids, which favors ROS production, reduces the hepatic expression of PPARα, and the loss of the transcriptional factor nuclear factor-erythroid factor 2-related factor 2 (Nrf2) activity [127]. PPARα forms a complex with the proinflammatory factor NF-κB, and the reduction of PPARα activates could activate NF-κB, thus leading to the steatotic and inflammatory responses in mice [128,129]. The inhibition of PPARα can directly aggravate oxidative stress and mitochondrial dysfunction [127,130]. In contrast, activation of PPARα and Nrf2, along with the deactivation of NF-κB could attenuate NAFLD induced by HFD [128,131]. Similarly, strategies to inhibit hepatic lipogenesis (via SREBP1) or to induce fatty acid β-oxidation (via PPARα) are associated with attenuated NF-κB-mediated inflammatory response and inhibited hepatic steatosis and NASH in mice [132,133]. Therefore, more studies are needed to examine whether the anti-oxidative stress activity of NAG-1/GDF15 is related to its directly or indirectly effect on PPARα or Nrf2 activation, and downregulation of NF-κB. In addition, whether the reduced AIM2 activation by NAG-1/GDF15 is a result of modulation of master regulators of lipid metabolism (SREBP1/PPARα) or a direct effect of NAG-1/GDF15 needs to be further examined.

Another unanswered question is the mechanisms by which NAG-1/GDF15 suppresses ROS and mitochondrial damage. It would be interesting to know whether NAG-1/GDF15 interacts with the Nrf2 signaling pathway to inhibit ROS production and induces the expression of the antioxidant genes, which all need to be further examined in future studies. Moreover, according to the GEO data analysis which revealed that NAG-1/GDF15 expression was significantly reduced in steatosis patients, but increased in NASH patients, large-scale studies are needed to evaluate the clinical importance of the different expression pattern of NAG-1/GDF15 during different stages of NAFLD. Whether a high level of NAG-1/GDF15 is desirable or not should be further examined in patients, particularly during the severe stage of NAFLD.

5. Conclusion

In conclusion, our study reveals the vital role of NAG-1/GDF15 in preventing hepatic steatosis in both HFD-induced *in vivo* and FFA-induced *in vitro* models of hepatic or cellular steatosis. Our study demonstrates that several mechanisms may explain how NAG-1/GDF15 elicits an inhibitory effect in the pathogenesis of hepatic steatosis. As depicted in Fig. 10, firstly, circulating or hepatic NAG-1/GDF15 may bind to unknown receptors of NAG-1/GDF15 on hepatocytes in an autocrine or paracrine manner, increases β-oxidation and lipolysis, reduces fatty acid uptake and *de novo* fatty acids synthesis, thus preventing excess lipid accumulation and subsequent hepatic steatosis in the liver.

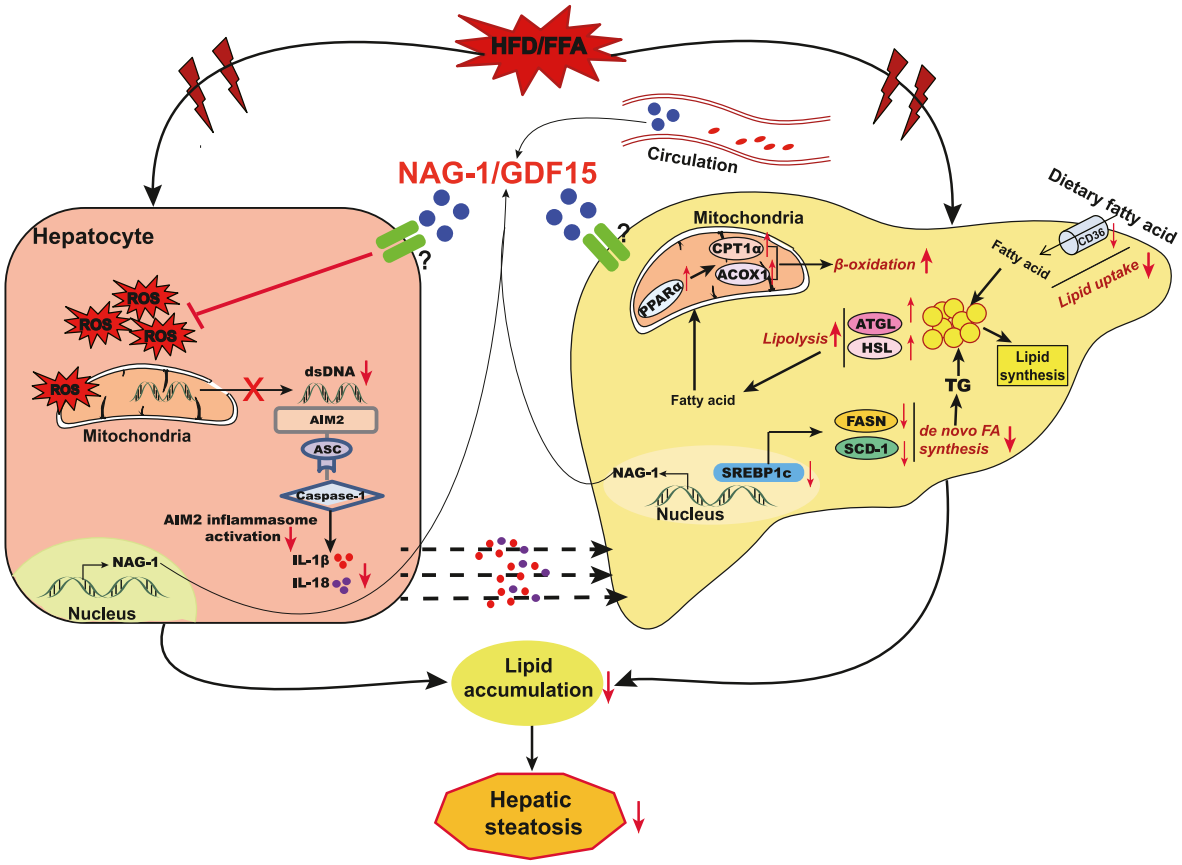

Fig. 10. Schematic model of NAG-1/GDF15-mediated inhibition of hepatic steatosis. NAG-1/GDF15 appears to inhibit hepatic steatosis through regulating lipid homeostasis and inhibiting AIM2 inflammasome activation upon HFD- or FFA-induced oxidative stress and dsDNA release in hepatocytes.

Secondly, we have uncovered a novel function of NAG-1/GDF15 in regulating mitochondrial function and oxidative stress. Our study reveals that NAG-1/GDF15 inhibits HFD- and FFA-induced oxidative stress and mitochondrial damage which reduces dsDNA release into the cytosol of hepatocytes, alleviates AIM2 inflammasome activation, and the release of IL-18 and IL-β. However, more studies are needed to clarify the association between these two mechanisms regulated by NAG-1/GDF15. Taken together, our findings provide new insight regarding the protective role of NAG-1/GDF15 in hepatic steatosis, suggesting an innovative therapeutic strategy for the treatment of NAFLD or related metabolic disorders through targeting NAG-1/GDF15. Moreover, inhibiting hepatic AIM2 and oxidative stress may be promising therapeutic targets for the treatment of NAFLD.

Author contributions

XW conceptualized, supervised, and provided funding for the project. YW, TE, and XW participated in the design of the study. YW performed majority of the experiments. CC, JC, TS, and HP helped with animal breeding, feeding experiment, and tissue processing. XL, QZ, and SC helped with animal necropsy and data recording. TE proofread the manuscript. XW and YW analyzed the data and wrote the manuscript. All authors read and approved the final manuscript.

Declaration of conflict of interest

The authors declare that they have no known competing financial interests or personal relationships that could have appeared to influence the work reported in this paper.

Acknowledgements

This study was supported by the National Natural Science Foundation of China (81400822; 81973521). We wish to thank Weimin Zhou, Chao Jiang, and Yuehan Qi at the animal facility for animal care at Zhejiang Chinese Medical University.

Appendix A. Supplementary data

Supplementary data to this article can be found online at https://doi.org/10.1016/j.redox.2022.102322.

References

[1] N. Chalasani, Z. Younossi, J.E. Lavine, M. Charlton, K. Cusi, M. Rinella, S. A. Harrison, E.M. Brunt, A.J. Sanyal, The diagnosis and management of nonalcoholic fatty liver disease: practice guidance from the American Association for the Study of Liver Diseases, Hepatology 67 (1) (2018) 328–357.
[2] E. Buzzetti, M. Pinzani, E.A. Tsochatzis, The multiple-hit pathogenesis of the non-alcoholic fatty liver disease (NAFLD), Metabolism 65 (8) (2016) 1038–1048.
[3] A. Takaki, D. Kawai, K. Yamamoto, Multiple hits, including oxidative stress, as pathogenesis and treatment target in non-alcoholic steatohepatitis (NASH), Int. J. Mol. Sci. 14 (10) (2013) 20704–20728.
[4] P. Ramadori, H. Drescher, S. Erschfeld, F. Schumacher, C. Berger, A. Fragoulis, J. Schenkel, T.W. Kensler, C.J. Wruck, C. Trautwein, D.C. Kroy, K.L. Streetz, Hepatocyte-specific Keap 1 deletion reduces liver steatosis but not inflammation during non-alcoholic steatohepatitis development, Free Radic. Biol. Med. 91 (2016) 114–126.
[5] V. Manne, P. Handa, K.V. Kowdley, Pathophysiology of nonalcoholic fatty liver disease/nonalcoholic steatohepatitis, Clin. Liver Dis. 22 (1) (2018) 23–37.
[6] A.P. Delli Bovi, F. Marciano, C. Mandato, M.A. Siano, M. Savoia, P. Vajro, Oxidative stress in non-alcoholic fatty liver disease. An updated mini review, Front. Med. 8 (2021), 595371.
[7] P.A. Kakimoto, A.J. Kowaltowski, Effects of high fat diets on rodent liver bioenergetics and oxidative imbalance, Redox Biol. 8 (2016) 216–225.

[8] A.M. Hetherington, C.G. Sawyez, E. Zilberman, A.M. Stoianov, D.L. Robson, N. M. Borradaile, Differential lipotoxic effects of palmitate and oleate in activated human hepatic stellate cells and epithelial hepatoma cells, Cell. Physiol. Biochem. 39 (4) (2016) 1648–1662.
[9] Y. Rotman, A.J. Sanyal, Current and upcoming pharmacotherapy for non-alcoholic fatty liver disease, Gut 66 (1) (2017) 180–190.
[10] D. Wang, E.A. Day, L.K. Townsend, D. Djordjevic, S.B. Jørgensen, G.R. Steinberg, GDF15: emerging biology and therapeutic applications for obesity and cardiometabolic disease, Nat. Rev. Endocrinol. 17 (10) (2021) 592–607.
[11] E.C. Hsiao, L.G. Koniaris, T. Zimmers-Koniaris, S.M. Sebald, T.V. Huynh, S.J. Lee, Characterization of growth-differentiation factor 15, a transforming growth factor beta superfamily member induced following liver injury, Mol. Cell Biol. 20 (10) (2000) 3742–3751.
[12] L.N. Lawton, M.F. Bonaldo, P.C. Jelenc, L. Qiu, S.A. Baumes, R.A. Marcelino, G. M. de Jesus, S. Wellington, J.A. Knowles, D. Warburton, S. Brown, M.B. Soares, Identification of a novel member of the TGF-beta superfamily highly expressed in human placenta, Gene 203 (1) (1997) 17–26.
[13] Y. Fujita, Y. Taniguchi, S. Shinkai, M. Tanaka, M. Ito, Secreted growth differentiation factor 15 as a potential biomarker for mitochondrial dysfunctions in aging and age-related disorders, Geriatr. Gerontol. Int. 16 (Suppl 1) (2016) 17–29.
[14] S.J. Baek, T. Eling, Growth differentiation factor 15 (GDF15): a survival protein with therapeutic potential in metabolic diseases, Pharmacol. Ther. 198 (2019) 46–58.
[15] L. Rochette, M. Zeller, Y. Cottin, C. Vergely, Insights into mechanisms of GDF15 and receptor GFRAL: therapeutic targets, Trends Endocrinol. Metabol. 31 (12) (2020) 939–951.
[16] J.B. Welsh, L.M. Sapinoso, S.G. Kern, D.A. Brown, T. Liu, A.R. Bauskin, R.L. Ward, N.J. Hawkins, D.I. Quinn, P.J. Russell, R.L. Sutherland, S.N. Breit, C.A. Moskaluk, H.F. Frierson Jr., G.M. Hampton, Large-scale delineation of secreted protein biomarkers overexpressed in cancer tissue and serum, Proc. Natl. Acad. Sci. U.S. A. 100 (6) (2003) 3410–3415.
[17] T. Kempf, A. Guba-Quint, J. Torgerson, M.C. Magnone, C. Haefliger, M. Bobadilla, K.C. Wollert, Growth differentiation factor 15 predicts future insulin resistance and impaired glucose control in obese nondiabetic individuals: results from the XENDOS trial, Eur. J. Endocrinol. 167 (5) (2012) 671–678.
[18] T. Kempf, S. von Haehling, T. Peter, T. Allhoff, M. Cicoira, W. Doehner, P. Ponikowski, G.S. Filippatos, P. Rozentryt, H. Drexler, S.D. Anker, K.C. Wollert, Prognostic utility of growth differentiation factor-15 in patients with chronic heart failure, J. Am. Coll. Cardiol. 50 (11) (2007) 1054–1060.
[19] V. Nair, C. Robinson-Cohen, M.R. Smith, K.A. Bellovich, Z.Y. Bhat, M. Bobadilla, F. Brosius, I.H. de Boer, L. Essioux, I. Formentini, C.A. Gadegbeku, D. Gipson, J. Hawkins, J. Himmelfarb, B. Kestenbaum, M. Kretzler, M.C. Magnone, K. Perumal, S. Steigerwalt, W. Ju, N. Bansal, Growth differentiation factor-15 and risk of CKD progression, J. Am. Soc. Nephrol. 28 (7) (2017) 2233–2240.
[20] X. Liu, X. Chi, Q. Gong, L. Gao, Y. Niu, X. Chi, M. Cheng, Y. Si, M. Wang, J. Zhong, J. Niu, W. Yang, Association of serum level of growth differentiation factor 15 with liver cirrhosis and hepatocellular carcinoma, PLoS One 10 (5) (2015), e0127518.
[21] E.S. Lee, S.H. Kim, H.J. Kim, K.H. Kim, B.S. Lee, B.J. Ku, Growth differentiation factor 15 predicts chronic liver disease severity, Gut Liver 11 (2) (2017) 276–282.
[22] S. Sarkar, S. Legere, I. Haidl, J. Marshall, J.B. MacLeod, C. Aguiar, S. Lutchmedial, A. Hassan, K.R. Brunt, P. Kienesberger, T. Pulinilkunnil, J.F. Légaré, Serum GDF15, a promising biomarker in obese patients undergoing heart surgery, Front. Cardiovasc. Med. 7 (2020) 103.
[23] I. Dostálová, T. Roubícek, M. Bártlová, M. Mráz, Z. Lacinová, D. Haluzíková, P. Kaválková, M. Matoulek, M. Kasalicky, M. Haluzík, Increased serum concentrations of macrophage inhibitory cytokine-1 in patients with obesity and type 2 diabetes mellitus: the influence of very low calorie diet, Eur. J. Endocrinol. 161 (3) (2009) 397–404.
[24] C.J. Petry, K.K. Ong, K.A. Burling, P. Barker, S.F. Goodburn, J.R.B. Perry, C. L. Acerini, I.A. Hughes, R.C. Painter, G.B. Afink, D.B. Dunger, S. O'Rahilly, Associations of vomiting and antiemetic use in pregnancy with levels of circulating GDF15 early in the second trimester: a nested case-control study, Wellcome, Open. Res. 3 (2018) 123.
[25] V.W. Tsai, L. Macia, C. Feinle-Bisset, R. Manandhar, A. Astrup, A. Raben, J. K. Lorenzen, P.T. Schmidt, F. Wiklund, N.L. Pedersen, L. Campbell, A. Kriketos, A. Xu, Z. Pengcheng, W. Jia, P.M. Curmi, C.N. Angstmann, K.K. Lee-Ng, H. P. Zhang, C.P. Marquis, Y. Husaini, C. Beglinger, S. Lin, H. Herzog, D.A. Brown, A. Sainsbury, S.N. Breit, Serum levels of human MIC-1/GDF15 vary in a diurnal pattern, do not display a profile suggestive of a satiety factor and are related to BMI, PLoS One 10 (7) (2015), e0133362.
[26] P.J. Emmerson, F. Wang, Y. Du, Q. Liu, R.T. Pickard, M.D. Gonciarz, T. Coskun, M.J. Hamang, D.K. Sindelar, K.K. Ballman, L.A. Foltz, A. Muppidi, J. Alsina-Fernandez, G.C. Barnard, J.X. Tang, X. Liu, X. Mao, R. Siegel, J.H. Sloan, P. J. Mitchell, B.B. Zhang, R.E. Gimeno, B. Shan, X. Wu, The metabolic effects of GDF15 are mediated by the orphan receptor GFRAL, Nat. Med. 23 (10) (2017) 1215–1219.
[27] L. Yang, C.C. Chang, Z. Sun, D. Madsen, H. Zhu, S.B. Padkjær, X. Wu, T. Huang, K. Hultman, S.J. Paulsen, J. Wang, A. Bugge, J.B. Frantzen, P. Nørgaard, J. F. Jeppesen, Z. Yang, A. Secher, H. Chen, X. Li, L.M. John, B. Shan, Z. He, X. Gao, J. Su, K.T. Hansen, W. Yang, S.B. Jørgensen, GFRAL is the receptor for GDF15 and is required for the anti-obesity effects of the ligand, Nat. Med. 23 (10) (2017) 1158–1166.
[28] S.E. Mullican, X. Lin-Schmidt, C.N. Chin, J.A. Chavez, J.L. Furman, A. A. Armstrong, S.C. Beck, V.J. South, T.Q. Dinh, T.D. Cash-Mason, C. R. Cavanaugh, S. Nelson, C. Huang, M.J. Hunter, S.M. Rangwala, GFRAL is the receptor for GDF15 and the ligand promotes weight loss in mice and nonhuman primates, Nat. Med. 23 (10) (2017) 1150–1157.
[29] K. Chrysovergis, X. Wang, J. Kosak, S.H. Lee, J.S. Kim, J.F. Foley, G. Travlos, S. Singh, S.J. Baek, T.E. Eling, NAG-1/GDF-15 prevents obesity by increasing thermogenesis, lipolysis and oxidative metabolism, Int. J. Obes. 38 (12) (2014) 1555–1564.
[30] H. Johnen, S. Lin, T. Kuffner, D.A. Brown, V.W. Tsai, A.R. Bauskin, L. Wu, G. Pankhurst, L. Jiang, S. Junankar, M. Hunter, W.D. Fairlie, N.J. Lee, R. F. Enriquez, P.A. Baldock, E. Corey, F.S. Apple, M.M. Murakami, E.J. Lin, C. Wang, M.J. During, A. Sainsbury, H. Herzog, S.N. Breit, Tumor-induced anorexia and weight loss are mediated by the TGF-beta superfamily cytokine MIC-1, Nat. Med. 13 (11) (2007) 1333–1340.
[31] Y. Xiong, K. Walker, X. Min, C. Hale, T. Tran, R. Komorowski, J. Yang, J. Davda, N. Nuanmanee, D. Kemp, X. Wang, H. Liu, S. Miller, K.J. Lee, Z. Wang, M. M. Véniant, Long-acting MIC-1/GDF15 molecules to treat obesity: evidence from mice to monkeys, Sci. Transl. Med. 9 (412) (2017), eaan8732.
[32] B.K. Koo, S.H. Um, D.S. Seo, S.K. Joo, J.M. Bae, J.H. Park, M.S. Chang, J.H. Kim, J. Lee, W.I. Jeong, W. Kim, Growth differentiation factor 15 predicts advanced fibrosis in biopsy-proven non-alcoholic fatty liver disease, Liver Int. 38 (4) (2018) 695–705.
[33] K.H. Kim, S.H. Kim, D.H. Han, Y.S. Jo, Y.H. Lee, M.S. Lee, Growth differentiation factor 15 ameliorates nonalcoholic steatohepatitis and related metabolic disorders in mice, Sci. Rep. 8 (1) (2018) 6789.
[34] S.G. Kang, M.J. Choi, S.B. Jung, H.K. Chung, J.Y. Chang, J.T. Kim, Y.E. Kang, J. H. Lee, H.J. Hong, S.M. Jun, H.J. Ro, J.M. Suh, H. Kim, J. Auwerx, H.S. Yi, M. Shong, Differential roles of GDF15 and FGF21 in systemic metabolic adaptation to the mitochondrial integrated stress response, iScience 24 (3) (2021), 102181.
[35] M. Zhang, W. Sun, J. Qian, Y. Tang, Fasting exacerbates hepatic growth differentiation factor 15 to promote fatty acid β-oxidation and ketogenesis via activating XBP1 signaling in liver, Redox Biol. 16 (2018) 87–96.
[36] Z. Zhang, X. Xu, W. Tian, R. Jiang, Y. Lu, Q. Sun, R. Fu, Q. He, J. Wang, Y. Liu, H. Yu, B. Sun, ARRB1 inhibits non-alcoholic steatohepatitis progression by promoting GDF15 maturation, J. Hepatol. 72 (5) (2020) 976–989.
[37] H. Guo, J.B. Callaway, J.P. Ting, Inflammasomes: mechanism of action, role in disease, and therapeutics, Nat. Med. 21 (7) (2015) 677–687.
[38] T. Fernandes-Alnemri, J.W. Yu, P. Datta, J. Wu, E.S. Alnemri, AIM2 activates the inflammasome and cell death in response to cytoplasmic DNA, Nature 458 (7237) (2009) 509–513.
[39] Z. Gong, X. Zhang, K. Su, R. Jiang, Z. Sun, W. Chen, E. Forno, E.S. Goetzman, J. Wang, H.H. Dong, P. Dutta, R. Muzumdar, Deficiency in AIM2 induces inflammation and adipogenesis in white adipose tissue leading to obesity and insulin resistance, Diabetologia 62 (12) (2019) 2325–2339.
[40] K. Deuteraiou, G. Kitas, A. Garyfallos, T. Dimitroulas, Novel insights into the role of inflammasomes in autoimmune and metabolic rheumatic diseases, Rheumatol. Int. 38 (8) (2018) 1345–1354.
[41] C. Martínez-Cardona, B. Lozano-Ruiz, V. Bachiller, G. Peiró, F. Algaba-Chueca, I. Gómez-Hurtado, J. Such, P. Zapater, R. Francés, J.M. González-Navajas, AIM2 deficiency reduces the development of hepatocellular carcinoma in mice, Int. J. Cancer 143 (11) (2018) 2997–3007.
[42] T. Csak, A. Pillai, M. Ganz, D. Lippai, J. Petrasek, J.K. Park, K. Kodys, A. Dolganiuc, E.A. Kurt-Jones, G. Szabo, Both bone marrow-derived and non-bone marrow-derived cells contribute to AIM2 and NLRP3 inflammasome activation in a MyD88-dependent manner in dietary steatohepatitis, Liver Int. 34 (9) (2014) 1402–1413.
[43] M. Ganz, T. Csak, G. Szabo, High fat diet feeding results in gender specific steatohepatitis and inflammasome activation, World, J. Gastroenterol. 20 (26) (2014) 8525–8534.
[44] L. Xu, J. Zhou, J. Che, H. Wang, W. Yang, W. Zhou, H. Zhao, Mitochondrial DNA enables AIM2 inflammasome activation and hepatocyte pyroptosis in nonalcoholic fatty liver disease, Am. J. Physiol. Gastrointest. Liver Physiol. 320 (6) (2021) G1034–g1044.
[45] H. Pan, Y. Wang, K. Na, Y. Wang, L. Wang, Z. Li, C. Guo, D. Guo, X. Wang, Autophagic flux disruption contributes to Ganoderma lucidum polysaccharide-induced apoptosis in human colorectal cancer cells via MAPK/ERK activation, Cell Death Dis. 10 (6) (2019) 456.
[46] S.J. Baek, R. Okazaki, S.H. Lee, J. Martinez, J.S. Kim, K. Yamaguchi, Y. Mishina, D.W. Martin, A. Shoieb, M.F. McEntee, T.E. Eling, Nonsteroidal anti-inflammatory drug-activated gene-1 over expression in transgenic mice suppresses intestinal neoplasia, Gastroenterology 131 (5) (2006) 1553–1560.
[47] M. Kadowaki, H. Yoshioka, H. Kamitani, T. Watanabe, P.A. Wade, T.E. Eling, DNA methylation-mediated silencing of nonsteroidal anti-inflammatory drug-activated gene (NAG-1/GDF15) in glioma cell lines, Int. J. Cancer 130 (2) (2012) 267–277.
[48] M.J. Gómez-Lechón, M.T. Donato, A. Martínez-Romero, N. Jiménez, J.V. Castell, J.E. O'Connor, A human hepatocellular in vitro model to investigate steatosis, Chem. Biol. Interact. 165 (2) (2007) 106–116.
[49] M. Ricchi, M.R. Odoardi, L. Carulli, C. Anzivino, S. Ballestri, A. Pinetti, L. I. Fantoni, F. Marra, M. Bertolotti, S. Banni, A. Lonardo, N. Carulli, P. Loria, Differential effect of oleic and palmitic acid on lipid accumulation and apoptosis in cultured hepatocytes, J. Gastroenterol. Hepatol. 24 (5) (2009) 830–840.
[50] N.C. Chavez-Tapia, N. Rosso, C. Tiribelli, In vitro models for the study of non-alcoholic fatty liver disease, Curr. Med. Chem. 18 (7) (2011) 1079–1084.
[51] O. Govaere, S. Cockell, D. Tiniakos, R. Queen, R. Younes, M. Vacca, L. Alexander, F. Ravaioli, J. Palmer, S. Petta, J. Boursier, C. Rosso, K. Johnson, K. Wonders, C. P. Day, M. Ekstedt, M. Orešič, R. Darlay, H.J. Cordell, F. Marra, A. Vidal-Puig,

P. Bedossa, J.M. Schattenberg, K. Clément, M. Allison, E. Bugianesi, V. Ratziu, A. K. Daly, Q.M. Anstee, Transcriptomic profiling across the nonalcoholic fatty liver disease spectrum reveals gene signatures for steatohepatitis and fibrosis, Sci. Transl. Med. 12 (527) (2020), eaba4448.
[52] M. Benedict, X. Zhang, Non-alcoholic fatty liver disease: an expanded review, World J. Hepatol. 9 (16) (2017) 715–732.
[53] L. Jiang, Q. Wang, Y. Yu, F. Zhao, P. Huang, R. Zeng, R.Z. Qi, W. Li, Y. Liu, Leptin contributes to the adaptive responses of mice to high-fat diet intake through suppressing the lipogenic pathway, PLoS One 4 (9) (2009), e6884.
[54] H. Jarvis, D. Craig, R. Barker, G. Spiers, D. Stow, Q.M. Anstee, B. Hanratty, Metabolic risk factors and incident advanced liver disease in non-alcoholic fatty liver disease (NAFLD): a systematic review and meta-analysis of population-based observational studies, PLoS Med. 17 (4) (2020), e1003100.
[55] L. Hodson, P.J. Gunn, The regulation of hepatic fatty acid synthesis and partitioning: the effect of nutritional state, Nat. Rev. Endocrinol. 15 (12) (2019) 689–700.
[56] G. Szabo, J. Petrasek, Inflammasome activation and function in liver disease, Nat. Rev. Gastroenterol. Hepatol. 12 (7) (2015) 387–400.
[57] S. Zilu, H. Qian, W. Haibin, G. Chenxu, L. Deshuai, L. Qiang, H. Linfeng, T. Jun, X. Minxuan, Effects of XIAP on high fat diet-induced hepatic steatosis: a mechanism involving NLRP3 inflammasome and oxidative stress, Aging (Albany NY) 11 (24) (2019) 12177–12201.
[58] T. Zheng, X. Yang, W. Li, Q. Wang, L. Chen, D. Wu, F. Bian, S. Xing, S. Jin, Salidroside attenuates high-fat diet-induced nonalcoholic fatty liver disease via AMPK-dependent TXNIP/NLRP3 pathway, Oxid. Med. Cell. Longev. (2018), 8597897, 2018.
[59] M.H. Kim, J.B. Seong, J.W. Huh, Y.C. Bae, H.S. Lee, D.S. Lee, Peroxiredoxin 5 ameliorates obesity-induced non-alcoholic fatty liver disease through the regulation of oxidative stress and AMP-activated protein kinase signaling, Redox Biol. 28 (2020), 101315.
[60] I.C.M. Simões, A. Fontes, P. Pinton, H. Zischka, M.R. Wieckowski, Mitochondria in non-alcoholic fatty liver disease, Int. J. Biochem. Cell Biol. 95 (2018) 93–99.
[61] X. Zhang, X. Wu, Q. Hu, J. Wu, G. Wang, Z. Hong, J. Ren, Mitochondrial DNA in liver inflammation and oxidative stress, Life Sci. 236 (2019), 116464.
[62] L.V. Yuzefovych, S.I. Musiyenko, G.L. Wilson, L.I. Rachek, Mitochondrial DNA damage and dysfunction, and oxidative stress are associated with endoplasmic reticulum stress, protein degradation and apoptosis in high fat diet-induced insulin resistance mice, PLoS One 8 (1) (2013), e54059.
[63] D.F. De Jesus, K. Orime, D. Kaminska, T. Kimura, G. Basile, C.H. Wang, L. Haertle, R. Riemens, N.K. Brown, J. Hu, V. Männistö, A.M. Silva, E. Dirice, Y.H. Tseng, T. Haaf, J. Pihlajamäki, R.N. Kulkarni, Parental metabolic syndrome epigenetically reprograms offspring hepatic lipid metabolism in mice, J. Clin. Invest. 130 (5) (2020) 2391–2407.
[64] M. Alves-Bezerra, D.E. Cohen, Triglyceride metabolism in the liver, Compr. Physiol. 8 (1) (2017) 1–8.
[65] A. Kotronen, T. Seppänen-Laakso, J. Westerbacka, T. Kiviluoto, J. Arola, A. L. Ruskeepää, M. Oresic, H. Yki-Järvinen, Hepatic stearoyl-CoA desaturase (SCD)-1 activity and diacylglycerol but not ceramide concentrations are increased in the nonalcoholic human fatty liver, Diabetes 58 (1) (2009) 203–208.
[66] C. Dorn, M.O. Riener, G. Kirovski, M. Saugspier, K. Steib, T.S. Weiss, E. Gäbele, G. Kristiansen, A. Hartmann, C. Hellerbrand, Expression of fatty acid synthase in nonalcoholic fatty liver disease, Int. J. Clin. Exp. Pathol. 3 (5) (2010) 505–514.
[67] M. Miyazaki, M.T. Flowers, H. Sampath, K. Chu, C. Otzelberger, X. Liu, J. M. Ntambi, Hepatic stearoyl-CoA desaturase-1 deficiency protects mice from carbohydrate-induced adiposity and hepatic steatosis, Cell Metabol. 6 (6) (2007) 484–496.
[68] M.M. Syed-Abdul, E.J. Parks, A.H. Gaballah, K. Bingham, G.M. Hammoud, G. Kemble, D. Buckley, W. McCulloch, C. Manrique-Acevedo, Fatty acid synthase inhibitor TVB-2640 reduces hepatic de Novo lipogenesis in males with metabolic abnormalities, Hepatology 72 (1) (2020) 103–118.
[69] C. Beysen, P. Schroeder, E. Wu, J. Brevard, M. Ribadeneira, W. Lu, K. Dole, T. O'Reilly, L. Morrow, M. Hompesch, M.K. Hellerstein, K. Li, L. Johansson, P. F. Kelly, Inhibition of fatty acid synthase with FT-4101 safely reduces hepatic de novo lipogenesis and steatosis in obese subjects with non-alcoholic fatty liver disease: results from two early-phase randomized trials, Diabetes Obes. Metabol. 23 (3) (2021) 700–710.
[70] H. Shimano, R. Sato, SREBP-regulated lipid metabolism: convergent physiology - divergent pathophysiology, Nat. Rev. Endocrinol. 13 (12) (2017) 710–730.
[71] Y.A. Moon, G. Liang, X. Xie, M. Frank-Kamenetsky, K. Fitzgerald, V. Koteliansky, M.S. Brown, J.L. Goldstein, J.D. Horton, The Scap/SREBP pathway is essential for developing diabetic fatty liver and carbohydrate-induced hypertriglyceridemia in animals, Cell Metabol. 15 (2) (2012) 240–246.
[72] P. Rada, Á. González-Rodríguez, C. García-Monzón, M. Valverde Á, Understanding lipotoxicity in NAFLD pathogenesis: is CD36 a key driver? Cell Death Dis. 11 (9) (2020) 802.
[73] C.G. Wilson, J.L. Tran, D.M. Erion, N.B. Vera, M. Febbraio, E.J. Weiss, Hepatocyte-specific disruption of CD36 attenuates fatty liver and improves insulin sensitivity in HFD-fed mice, Endocrinology 157 (2) (2016) 570–585.
[74] L. Barbier-Torres, K.A. Fortner, P. Iruzubieta, T.C. Delgado, E. Giddings, Y. Chen, D. Champagne, D. Fernández-Ramos, D. Mestre, B. Gomez-Santos, M. Varela-Rey, V.G. de Juan, P. Fernández-Tussy, I. Zubiete-Franco, C. García-Monzón, Á. González-Rodríguez, D. Oza, F. Valença-Pereira, Q. Fang, J. Crespo, P. Aspichueta, F. Tremblay, B.C. Christensen, J. Anguita, M.L. Martínez-Chantar, M. Rincón, Silencing hepatic MCJ attenuates non-alcoholic fatty liver disease (NAFLD) by increasing mitochondrial fatty acid oxidation, Nat. Commun. 11 (1) (2020) 3360.
[75] G. Naguib, N. Morris, S. Yang, N. Fryzek, V. Haynes-Williams, W.A. Huang, J. Norman-Wheeler, Y. Rotman, Dietary fatty acid oxidation is decreased in non-alcoholic fatty liver disease: a palmitate breath test study, Liver Int. 40 (3) (2020) 590–597.
[76] S.H. Koo, Nonalcoholic fatty liver disease: molecular mechanisms for the hepatic steatosis, Clin. Mol. Hepatol. 19 (3) (2013) 210–215.
[77] D.H. Ipsen, J. Lykkesfeldt, P. Tveden-Nyborg, Molecular mechanisms of hepatic lipid accumulation in non-alcoholic fatty liver disease, Cell. Mol. Life Sci. 75 (18) (2018) 3313–3327.
[78] M. Shum, J. Ngo, O.S. Shirihai, M. Liesa, Mitochondrial oxidative function in NAFLD: friend or foe? Mol. Metabol. 50 (2021), 101134.
[79] A. Montagner, A. Polizzi, E. Fouché, S. Ducheix, Y. Lippi, F. Lasserre, V. Barquissau, M. Régnier, C. Lukowicz, F. Benhamed, A. Iroz, J. Bertrand-Michel, T. Al Saati, P. Cano, L. Mselli-Lakhal, G. Mithieux, F. Rajas, S. Lagarrigue, T. Pineau, N. Loiseau, C. Postic, D. Langin, W. Wahli, H. Guillou, Liver PPARα is crucial for whole-body fatty acid homeostasis and is protective against NAFLD, Gut 65 (7) (2016) 1202–1214.
[80] M. Régnier, A. Polizzi, Y. Lippi, E. Fouché, G. Michel, C. Lukowicz, S. Smati, A. Marrot, F. Lasserre, C. Naylies, A. Batut, F. Viars, J. Bertrand-Michel, C. Postic, N. Loiseau, W. Wahli, H. Guillou, A. Montagner, Insights into the role of hepatocyte PPARα activity in response to fasting, Mol. Cell. Endocrinol. 471 (2018) 75–88.
[81] A. Tailleux, K. Wouters, B. Staels, Roles of PPARs in NAFLD: potential therapeutic targets, Biochim. Biophys. Acta 1821 (5) (2012) 809–818.
[82] W.P. Esler, K.K. Bence, Metabolic targets in nonalcoholic fatty liver disease, Cell. Mol. Gastroenterol. Hepatol. 8 (2) (2019) 247–267.
[83] M. Régnier, A. Polizzi, S. Smati, C. Lukowicz, A. Fougerat, Y. Lippi, E. Fouché, F. Lasserre, C. Naylies, C. Bétoulières, V. Barquissau, E. Mouisel, J. Bertrand-Michel, A. Batut, T.A. Saati, C. Canlet, M. Tremblay-Franco, S. Ellero-Simatos, D. Langin, C. Postic, W. Wahli, N. Loiseau, H. Guillou, A. Montagner, Hepatocyte-specific deletion of Pparα promotes NAFLD in the context of obesity, Sci. Rep. 10 (1) (2020) 6489.
[84] W. Xiao, M. Ren, C. Zhang, S. Li, W. An, Amelioration of nonalcoholic fatty liver disease by hepatic stimulator substance via preservation of carnitine palmitoyl transferase-1 activity, Am. J. Physiol. Cell Physiol. 309 (4) (2015) C215–C227.
[85] M.E. Moreno-Fernandez, D.A. Giles, T.E. Stankiewicz, R. Sheridan, R. Karns, M. Cappelletti, K. Lampe, R. Mukherjee, C. Sina, A. Sallese, J.P. Bridges, S. P. Hogan, B.J. Aronow, K. Hoebe, S. Divanovic, Peroxisomal β-oxidation regulates whole body metabolism, inflammatory vigor, and pathogenesis of nonalcoholic fatty liver disease, JCI insight 3 (6) (2018), e93626.
[86] C.D. Fuchs, T. Claudel, M. Trauner, Role of metabolic lipases and lipolytic metabolites in the pathogenesis of NAFLD, Trends Endocrinol. Metabol. 25 (11) (2014) 576–585.
[87] J.W. Wu, S.P. Wang, F. Alvarez, S. Casavant, N. Gauthier, L. Abed, K.G. Soni, G. Yang, G.A. Mitchell, Deficiency of liver adipose triglyceride lipase in mice causes progressive hepatic steatosis, Hepatology 54 (1) (2011) 122–132.
[88] B.N. Reid, G.P. Ables, O.A. Otlivanchik, G. Schoiswohl, R. Zechner, W.S. Blaner, I. J. Goldberg, R.F. Schwabe, S.C. Chua Jr., L.S. Huang, Hepatic overexpression of hormone-sensitive lipase and adipose triglyceride lipase promotes fatty acid oxidation, stimulates direct release of free fatty acids, and ameliorates steatosis, J. Biol. Chem. 283 (19) (2008) 13087–13099.
[89] J.Y. Hsu, S. Crawley, M. Chen, D.A. Ayupova, D.A. Lindhout, J. Higbee, A. Kutach, W. Joo, Z. Gao, D. Fu, C. To, K. Mondal, B. Li, A. Kekatpure, M. Wang, T. Laird, G. Horner, J. Chan, M. McEntee, M. Lopez, D. Lakshminarasimhan, A. White, S.P. Wang, J. Yao, J. Yie, H. Matern, M. Solloway, R. Haldankar, T. Parsons, J. Tang, W.D. Shen, Y. Alice Chen, H. Tian, B.B. Allan, Non-homeostatic body weight regulation through a brainstem-restricted receptor for GDF15, Nature 550 (7675) (2017) 255–259.
[90] H.K. Chung, D. Ryu, K.S. Kim, J.Y. Chang, Y.K. Kim, H.S. Yi, S.G. Kang, M.J. Choi, S.E. Lee, S.B. Jung, M.J. Ryu, S.J. Kim, G.R. Kweon, H. Kim, J.H. Hwang, C. H. Lee, S.J. Lee, C.E. Wall, M. Downes, R.M. Evans, J. Auwerx, M. Shong, Growth differentiation factor 15 is a myomitokine governing systemic energy homeostasis, J. Cell Biol. 216 (1) (2017) 149–165.
[91] M.J. Choi, S.B. Jung, S.E. Lee, S.G. Kang, J.H. Lee, M.J. Ryu, H.K. Chung, J. Y. Chang, Y.K. Kim, H.J. Hong, H. Kim, H.J. Kim, C.H. Lee, A. Mardinoglu, H. S. Yi, M. Shong, An adipocyte-specific defect in oxidative phosphorylation increases systemic energy expenditure and protects against diet-induced obesity in mouse models, Diabetologia 63 (4) (2020) 837–852.
[92] M. Ost, C. Igual Gil, V. Coleman, S. Keipert, S. Efstathiou, V. Vidic, M. Weyers, S. Klaus, Muscle-derived GDF15 drives diurnal anorexia and systemic metabolic remodeling during mitochondrial stress, EMBO Rep. 21 (3) (2020), e48804.
[93] D. Aguilar-Recarte, E. Barroso, A. Gumà, J. Pizarro-Delgado, L. Peña, M. Ruart, X. Palomer, W. Wahli, M. Vázquez-Carrera, GDF15 mediates the metabolic effects of PPARβ/δ by activating AMPK, Cell Rep. 36 (6) (2021), 109501.
[94] K.H. Kim, M.S. Lee, GDF15 as a central mediator for integrated stress response and a promising therapeutic molecule for metabolic disorders and NASH, Biochim. Biophys. Acta Gen. Subj. 1865 (3) (2021), 129834.
[95] A. Artz, S. Butz, D. Vestweber, GDF-15 inhibits integrin activation and mouse neutrophil recruitment through the ALK-5/TGF-βRII heterodimer, Blood 128 (4) (2016) 529–541.
[96] M. Guillaume, E. Riant, A. Fabre, I. Raymond-Letron, M. Buscato, M. Davezac, B. Tramunt, A. Montagner, S. Smati, R. Zahreddine, G. Palierne, M.C. Valera, H. Guillou, F. Lenfant, K. Unsicker, R. Metivier, C. Fontaine, J.F. Arnal, P. Gourdy, Selective liver estrogen receptor α modulation prevents steatosis, diabetes, and obesity through the anorectic growth differentiation factor 15 hepatokine in mice, Hepatol. Commun. 3 (7) (2019) 908–924.

[97] J. Wischhusen, I. Melero, W.H. Fridman, Growth/differentiation factor-15 (GDF-15): from biomarker to novel targetable immune checkpoint, Front. Immunol. 11 (2020) 951.
[98] Y. Myojin, H. Hikita, M. Sugiyama, Y. Sasaki, K. Fukumoto, S. Sakane, Y. Makino, N. Takemura, R. Yamada, M. Shigekawa, T. Kodama, R. Sakamori, S. Kobayashi, T. Tatsumi, H. Suemizu, H. Eguchi, N. Kokudo, M. Mizokami, T. Takehara, Hepatic stellate cells in hepatocellular carcinoma promote tumor growth via growth differentiation factor 15 production, Gastroenterology 160 (5) (2021) 1741–1754, e16.
[99] C. Lebeaupin, D. Vallée, Y. Hazari, C. Hetz, E. Chevet, B. Bailly-Maitre, Endoplasmic reticulum stress signalling and the pathogenesis of non-alcoholic fatty liver disease, J. Hepatol. 69 (4) (2018) 927–947.
[100] K.T. Pfaffenbach, C.L. Gentile, A.M. Nivala, D. Wang, Y. Wei, M.J. Pagliassotti, Linking endoplasmic reticulum stress to cell death in hepatocytes: roles of C/EBP homologous protein and chemical chaperones in palmitate-mediated cell death, Am. J. Physiol. Endocrinol. Metab. 298 (5) (2010) E1027–E1035.
[101] H. Yang, S.H. Park, H.J. Choi, Y. Moon, The integrated stress response-associated signals modulates intestinal tumor cell growth by NSAID-activated gene 1 (NAG-1/MIC-1/PTGF-beta), Carcinogenesis 31 (4) (2010) 703–711.
[102] H. Zheng, Y. Wu, T. Guo, F. Liu, Y. Xu, S. Cai, Hypoxia induces growth differentiation factor 15 to promote the metastasis of colorectal cancer via PERK-eIF2α signaling, BioMed Res. Int. 2020 (2020), 5958272.
[103] L. L'Homme, B.P. Sermikli, B. Staels, J. Piette, S. Legrand-Poels, D. Dombrowicz, Saturated fatty acids promote GDF15 expression in human macrophages through the PERK/eIF2/CHOP signaling pathway, Nutrients 12 (12) (2020) 3771.
[104] D. Li, H. Zhang, Y. Zhong, Hepatic GDF15 is regulated by CHOP of the unfolded protein response and alleviates NAFLD progression in obese mice, Biochem. Biophys. Res. Commun. 498 (3) (2018) 388–394.
[105] S. Yatsuga, Y. Fujita, A. Ishii, Y. Fukumoto, H. Arahata, T. Kakuma, T. Kojima, M. Ito, M. Tanaka, R. Saiki, Y. Koga, Growth differentiation factor 15 as a useful biomarker for mitochondrial disorders, Ann. Neurol. 78 (5) (2015) 814–823.
[106] J. Zhang, Y. Zhao, C. Xu, Y. Hong, H. Lu, J. Wu, Y. Chen, Association between serum free fatty acid levels and nonalcoholic fatty liver disease: a cross-sectional study, Sci. Rep. 4 (2014) 5832.
[107] J. Pan, Z. Ou, C. Cai, P. Li, J. Gong, X.Z. Ruan, K. He, Fatty acid activates NLRP3 inflammasomes in mouse Kupffer cells through mitochondrial DNA release, Cell. Immunol. 332 (2018) 111–120.
[108] R.W. Grant, V.D. Dixit, Mechanisms of disease: inflammasome activation and the development of type 2 diabetes, Front. Immunol. 4 (2013) 50.
[109] L.D. Cunha, A.L.N. Silva, J.M. Ribeiro, D.P.A. Mascarenhas, G.F.S. Quirino, L. L. Santos, R.A. Flavell, D.S. Zamboni, AIM2 engages active but unprocessed caspase-1 to induce noncanonical activation of the NLRP3 inflammasome, Cell Rep. 20 (4) (2017) 794–805.
[110] H. Thomas, NAFLD: a critical role for the NLRP3 inflammasome in NASH, Nat. Rev. Gastroenterol. Hepatol. 14 (4) (2017) 197.
[111] R. Stienstra, L.A. Joosten, T. Koenen, B. van Tits, J.A. van Diepen, S.A. van den Berg, P.C. Rensen, P.J. Voshol, G. Fantuzzi, A. Hijmans, S. Kersten, M. Müller, W. B. van den Berg, N. van Rooijen, M. Wabitsch, B.J. Kullberg, J.W. van der Meer, T. Kanneganti, C.J. Tack, M.G. Netea, The inflammasome-mediated caspase-1 activation controls adipocyte differentiation and insulin sensitivity, Cell Metabol. 12 (6) (2010) 593–605.
[112] R. Stienstra, J.A. van Diepen, C.J. Tack, M.H. Zaki, F.L. van de Veerdonk, D. Perera, G.A. Neale, G.J. Hooiveld, A. Hijmans, I. Vroegrijk, S. van den Berg, J. Romijn, P.C. Rensen, L.A. Joosten, M.G. Netea, T.D. Kanneganti, Inflammasome is a central player in the induction of obesity and insulin resistance, Proc. Natl. Acad. Sci. U.S.A. 108 (37) (2011) 15324–15329.
[113] J. Henao-Mejia, E. Elinav, C. Jin, L. Hao, W.Z. Mehal, T. Strowig, C.A. Thaiss, A. L. Kau, S.C. Eisenbarth, M.J. Jurczak, J.P. Camporez, G.I. Shulman, J.I. Gordon, H.M. Hoffman, R.A. Flavell, Inflammasome-mediated dysbiosis regulates progression of NAFLD and obesity, Nature 482 (7384) (2012) 179–185.
[114] A. Wree, M.D. McGeough, C.A. Peña, M. Schlattjan, H. Li, M.E. Inzaugarat, K. Messer, A. Canbay, H.M. Hoffman, A.E. Feldstein, NLRP3 inflammasome activation is required for fibrosis development in NAFLD, J. Mol. Med. (Berl.) 92 (10) (2014) 1069–1082.
[115] T. Csak, M. Ganz, J. Pespisa, K. Kodys, A. Dolganiuc, G. Szabo, Fatty acid and endotoxin activate inflammasomes in mouse hepatocytes that release danger signals to stimulate immune cells, Hepatology 54 (1) (2011) 133–144.
[116] A.R. Mridha, A. Wree, A.A.B. Robertson, M.M. Yeh, C.D. Johnson, D.M. Van Rooyen, F. Haczeyni, N.C. Teoh, C. Savard, G.N. Ioannou, S.L. Masters, K. Schroder, M.A. Cooper, A.E. Feldstein, G.C. Farrell, NLRP3 inflammasome blockade reduces liver inflammation and fibrosis in experimental NASH in mice, J. Hepatol. 66 (5) (2017) 1037–1046.
[117] G. Yang, H.E. Lee, J.Y. Lee, A pharmacological inhibitor of NLRP3 inflammasome prevents non-alcoholic fatty liver disease in a mouse model induced by high fat diet, Sci. Rep. 6 (2016) 24399.
[118] B. Vandanmagsar, Y.H. Youm, A. Ravussin, J.E. Galgani, K. Stadler, R.L. Mynatt, E. Ravussin, J.M. Stephens, V.D. Dixit, The NLRP3 inflammasome instigates obesity-induced inflammation and insulin resistance, Nat. Med. 17 (2) (2011) 179–188.
[119] X. Wang, K. Chrysovergis, J. Kosak, T.E. Eling, Lower NLRP3 inflammasome activity in NAG-1 transgenic mice is linked to a resistance to obesity and increased insulin sensitivity, Obesity 22 (5) (2014) 1256–1263.
[120] P. Kumari, A.J. Russo, S. Shivcharan, V.A. Rathinam, AIM2 in health and disease: inflammasome and beyond, Immunol. Rev. 297 (1) (2020) 83–95.
[121] B.R. Sharma, R. Karki, T.D. Kanneganti, Role of AIM2 inflammasome in inflammatory diseases, cancer and infection, Eur. J. Immunol. 49 (11) (2019) 1998–2011.
[122] B. Lozano-Ruiz, J.M. González-Navajas, The emerging relevance of AIM2 in liver disease, Int. J. Mol. Sci. 21 (18) (2020) 6535.
[123] Y.G. Cataño Cañizales, E.E. Uresti Rivera, R.E. García Jacobo, D.P. Portales Perez, B. Yadira, J.G. Rodriguez Rivera, R.G. Amaro, J.A. Enciso Moreno, M.H. García Hernández, Increased levels of AIM2 and circulating mitochondrial DNA in type 2 diabetes, Iran, J. Immunol. 15 (2) (2018) 142–155.
[124] B. Nair, L.R. Nath, Inevitable role of TGF-β1 in progression of nonalcoholic fatty liver disease, J. Recept. Signal Transduct. Res. 40 (3) (2020) 195–200.
[125] L. Zeng, W.J. Tang, J.J. Yin, B.J. Zhou, Signal transductions and nonalcoholic fatty liver: a mini-review, Int. J. Clin. Exp. Med. 7 (7) (2014) 1624–1631.
[126] M. Verdelho Machado, A.M. Diehl, The hedgehog pathway in nonalcoholic fatty liver disease, Crit. Rev. Biochem. Mol. Biol. 53 (3) (2018) 264–278.
[127] M. Ortiz, S.A. Soto-Alarcón, P. Orellana, A. Espinosa, C. Campos, S. López-Arana, M.A. Rincón, P. Illesca, R. Valenzuela, L.A. Videla, Suppression of high-fat diet-induced obesity-associated liver mitochondrial dysfunction by docosahexaenoic acid and hydroxytyrosol co-administration, Dig. Liver Dis. 52 (8) (2020) 895–904.
[128] R. Valenzuela, P. Illesca, F. Echeverría, A. Espinosa, M. Rincón-Cervera, M. Ortiz, M.C. Hernandez-Rodas, A. Valenzuela, L.A. Videla, Molecular adaptations underlying the beneficial effects of hydroxytyrosol in the pathogenic alterations induced by a high-fat diet in mouse liver: PPAR-α and Nrf2 activation, and NF-κB down-regulation, Food Funct. 8 (4) (2017) 1526–1537.
[129] G. Tapia, R. Valenzuela, A. Espinosa, P. Romanque, C. Dossi, D. Gonzalez-Mañán, L.A. Videla, A. D'Espessailles, N-3 long-chain PUFA supplementation prevents high fat diet induced mouse liver steatosis and inflammation in relation to PPAR-α upregulation and NF-κB DNA binding abrogation, Mol. Nutr. Food Res. 58 (6) (2014) 1333–1341.
[130] M.A. Abdelmegeed, S.H. Yoo, L.E. Henderson, F.J. Gonzalez, K.J. Woodcroft, B. J. Song, PPARalpha expression protects male mice from high fat-induced nonalcoholic fatty liver, J. Nutr. 141 (4) (2011) 603–610.
[131] F. Echeverría, R. Valenzuela, A. Bustamante, D. Álvarez, M. Ortiz, S.A. Soto-Alarcon, P. Muñoz, A. Corbari, L.A. Videla, Attenuation of high-fat diet-induced rat liver oxidative stress and steatosis by combined hydroxytyrosol- (HT-) eicosapentaenoic acid supplementation mainly relies on HT, Oxid. Med. Cell. Longev. (2018), 5109503, 2018.
[132] O. Rom, G. Xu, Y. Guo, Y. Zhu, H. Wang, J. Zhang, Y. Fan, W. Liang, H. Lu, Y. Liu, M. Aviram, Z. Liu, S. Kim, W. Liu, X. Wang, Y.E. Chen, L. Villacorta, Nitro-fatty acids protect against steatosis and fibrosis during development of nonalcoholic fatty liver disease in mice, EBioMedicine 41 (2019) 62–72.
[133] O. Rom, Y. Liu, Z. Liu, Y. Zhao, J. Wu, A. Ghrayeb, L. Villacorta, Y. Fan, L. Chang, L. Wang, C. Liu, D. Yang, J. Song, J.C. Rech, Y. Guo, H. Wang, G. Zhao, W. Liang, Y. Koike, H. Lu, T. Koike, T. Hayek, S. Pennathur, C. Xi, B. Wen, D. Sun, M. T. Garcia-Barrio, M. Aviram, E. Gottlieb, I. Mor, W. Liu, J. Zhang, Y.E. Chen, Glycine-based treatment ameliorates NAFLD by modulating fatty acid oxidation, glutathione synthesis, and the gut microbiome, Sci. Transl. Med. 12 (572) (2020) eaaz2841.